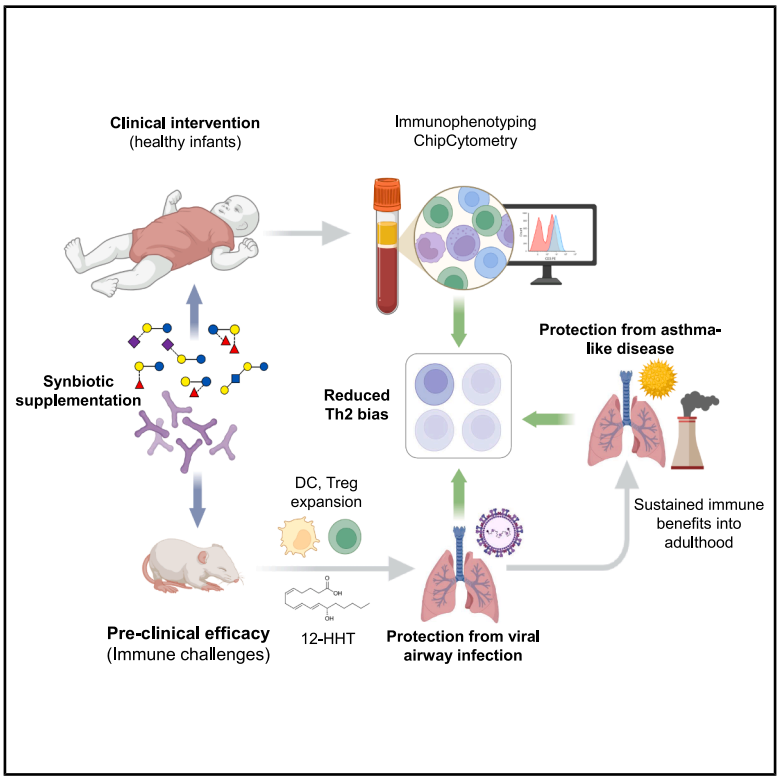
Cell Reports
Medicine

Article

Early-life immune imprinting by a *B. infantis*-HMO synbiotic shapes infant immune signatures and protects against experimental respiratory disease

Graphical abstract



Authors

Ridwan B. Rashid, Cheong Kwong Chung, Patricia Namubiru, ..., Jean-Charles Picaud, Simon Phipps, Mario Noti

Correspondence

simon.phipps@qimbr.edu.au (S.P.), mario.noti@rd.nestle.com (M.N.)

In brief

Rashid et al. report that an infant-type *Bifidobacterium infantis*-HMO synbiotic shapes immune signatures and reduces Th2 bias in formula-fed infants toward a breastfed-like profile. In experimental models, it protects against bronchiolitis and confers lasting immune effects into adulthood, associated with increased 12-HHT, a lipid mediator sufficient to promote disease tolerance.

Highlights

- Synbiotic supplementation reduces Th2 abundance in infant blood
- Synbiotic protects neonatal mice from sLRI and confers lasting immune benefits
- Synbiotic increases 12-HHT, linked to improved infection outcomes
- Oral 12-HHT supplementation phenocopies synbiotic-mediated protection from sLRI

Rashid et al., 2026, Cell Reports Medicine 7, 102935
August 18, 2026 © 2026 Published by Elsevier Inc.
https://doi.org/10.1016/j.xcrm.2026.102935

CellPress

Cell Reports Medicine

CellPress
OPEN ACCESS

Article

Early-life immune imprinting by a *B. infantis*-HMO synbiotic shapes infant immune signatures and protects against experimental respiratory disease

Ridwan B. Rashid,[1,2] Cheong Kwong Chung,[3] Patricia Namubiru,[1,2] Tufael Ahmed,[1,4] CLARA Study Group, Daniel R. Howard,[1,2] Ismail Sebina,[1] Tyler Wilkins,[1,4] Md. Sohel Rana,[1,4] Joshua P. Morrow,[5] Darren J. Creek,[5] Janne Marie Moll,[6] Karine Vidal,[3] Cecilia Fumero,[7] Luca Lavalle,[7] Dominick Maes,[8] Nicholas P. Hays,[9] Irma Silva-Zolezzi,[9] Elizabeth Forbes-Blom,[9] Norbert Sprenger,[3] Jean-Charles Picaud,[10] Simon Phipps,[1,2,4,11,12,*] and Mario Noti[3,11,*]

[1]QIMR Berghofer Medical Research Institute, Herston, QLD 4006, Australia
[2]School of Biomedical Sciences, Faculty of Medicine, The University of Queensland, Brisbane, QLD 4072, Australia
[3]Société des Produits Nestlé S.A., Nestlé Research, Nestlé Institute of Health Sciences, 1000 Lausanne, Switzerland
[4]School of Biomedical Sciences, Faculty of Health, Queensland University of Technology, Brisbane, QLD 4000, Australia
[5]Monash Instit4ute of Pharmaceutical Sciences, Parkville, VIC 3052, Australia
[6]Cmbio, 2100 Copenhagen, Denmark
[7]Société des Produits Nestlé S.A., Nestlé Research, Clinical Research Unit, 1000 Lausanne, Switzerland
[8]Société des Produits Nestlé S.A., Nestlé Product Technology Centre - Nutrition, 3510 Konolfingen, Switzerland
[9]Société des Produits Nestlé S.A., Nestlé Product Technology Center - Nutrition, 1800 Vevey, Switzerland
[10]Department of Neonatology, Hôpital de La Croix-Rousse, 69004 Lyon, France and CarMen Laboratory, INSERM, INRA, Université Claude Bernard Lyon 1, Pierre-Bénite, 69310 Lyon, France
[11]These authors contributed equally
[12]Lead contact
*Correspondence: simon.phipps@qimbr.edu.au (S.P.), mario.noti@rd.nestle.com (M.N.)
https://doi.org/10.1016/j.xcrm.2026.102935

SUMMARY

Early microbial colonization influences immune development, with lower abundance of human milk oligosaccharide (HMO)-utilizing bifidobacteria linked to immune-related disorder risk. Here, we demonstrate that synbiotic supplementation with *Bifidobacterium infantis* (LMG 11588) and a blend of six structurally diverse HMOs plus *Bifidobacterium lactis* (CNCM I-3446) altered gut microbiome composition, changed systemic immune cell-networks, and reduced persistence of a T helper 2 (Th2) bias in formula-fed infants, following a pattern observed in breastfed infants. In preclinical models, synbiotic reduces lower respiratory tract infection (LRI) severity and aberrant type-2 immune responses and confers lasting immune benefits into adulthood. These effects are associated with changes in the circulating metabolome, including increased 12(S)-hydroxyheptadecatrienoic acid (12-HHT), which correlates with improved infection outcomes and phenocopies synbiotic-mediated protection when administered orally. Together, these findings indicate that infant-type synbiotic supplementation during a critical early-life window can imprint immune function and promote disease tolerance.

INTRODUCTION

Newborns face major challenges during the transition from the protected intrauterine environment to the outside world.[1,2] This requires the immune system to defend against pathogens while remaining tolerant to beneficial microbes and essential nutrients.[3] Increasing evidence supports the existence of critical early-life windows that favor healthy immune development.[4,5] Factors such as maternal health, mode of birth and feeding, antibiotic exposure, and environmental influences shape early microbial colonization and long-term immune function.[6] Bifidobacteria, among the first infant gut colonizers, utilize human milk oligosaccharides (HMOs) to drive microbiota maturation and support immune development.[6,7] These infant-type bifidobacteria act as ecosystem engineers by enabling microbial succession via metabolic cross-feeding.[8] Disruption of these highly dynamic colonization patterns can impair coordinated microbiome-host interactions, alter immune trajectories, and increase disease susceptibility across the life course.[9–11] Consistently, severe lower respiratory tract infections (sLRIs) in infancy are linked to impaired lung function, later chronic respiratory diseases (e.g., asthma), and increased all-cause mortality.[12,13]

Human milk represents a unique source of nutrition, providing a selective advantage for the colonization of specific infant-type bifidobacteria specialized to metabolize HMOs.[14,15] Among these, *Bifidobacterium longum* subspecies *infantis* (*B. infantis*) is highly specialized to metabolize structurally diverse HMOs to produce a range of metabolites, which in turn may benefit the

This is an open access article under the CC BY-NC-ND license (http://creativecommons.org/licenses/by-nc-nd/4.0/).

infant by modulating immune function and disease tolerance in early life.[16,17] Observational studies have identified a link between the abundance of *B. infantis* in early life and atopic disorders, with lower abundances representing a risk factor for developing chronic inflammatory disease.[18] In line with the above, low abundance of *B. infantis* in infancy correlates with enteric inflammation, and supplementation of *B. infantis* has been reported to silence T helper 2 (Th2) and Th17 immune responses in breastfed infants.[6] This effect was most pronounced in exclusively breastfed infants, providing further evidence for the hypothesis of a synbiotic effect of the combination of HMOs and *B. infantis* on immune system modulation.[19] Gaining a deeper understanding of coordinated microbiome-immune interactions in early life will enhance/accelerate biotic intervention strategies to support appropriate immune development and resilience against risk factors linked to the onset of chronic inflammatory disorders.

Here, we assessed the impact of supplementation with a specific synbiotic blend in early life on systemic immune cell profiles in a sub-cohort of a randomized controlled double-blind infant formula trial.[20] For this, we used a formulation including an infant-type synbiotic tailored to infants and young children reflecting the composition of HMOs in breast milk and supporting the development of the gut microbiota in early life, in combination with an infant-type *Bifidobacterium*, *B. infantis* (specialized to metabolize HMOs), + *B. lactis* known for their immunomodulatory properties. We demonstrate that supplementation with this infant-type synbiotic changes systemic immune cell networks and reduces a Th2 bias in formula fed infants—to more closely follow the pattern observed in exclusively breastfed infants enrolled as a non-randomized reference group. To gain further mechanistic insight, we evaluated the impact of early-life synbiotic supplementation on preclinical models of respiratory infection and allergic airway inflammation. We find that synbiotic supplementation improves disease tolerance toward an sLRI associated with aberrant Th2 responses in early life and reduces susceptibility to experimental asthma later in life. The improved infection and allergy outcomes following synbiotic supplementation associate with significant changes in the levels of systemic metabolites and the expansion of immunoregulatory plasmacytoid dendritic cells (pDCs) and regulatory T cell (Treg) responses. Together, these findings support the concept that during a critical developmental window in early life an infant-type synbiotic has the capacity to shape immune system imprinting and prevent the development of a severe infection and subsequent asthma via the promotion of disease tolerance.

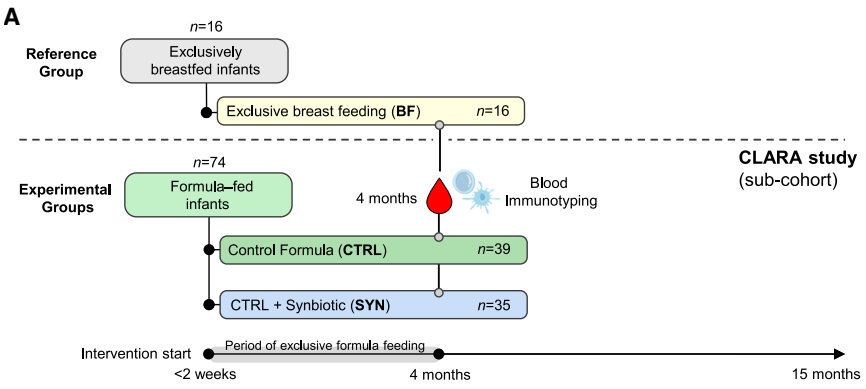
RESULTS

Supplementation with an infant-type synbiotic modulates systemic immune signatures in infants

In a sub-cohort of a randomized, controlled, double-blind multicenter European infant formula trial (clinicaltrials.gov, NCT04962594,[20]), we assessed the impact of early-life supplementation with an infant-type synbiotic consisting of *B. infantis* (LMG 11588) and a blend of structurally diverse HMOs plus *Bifidobacterium lactis* (*B. lactis*, CNCM I-3446) on systemic immune signatures and immune cell networks in the first 4 months of life. For the full study, healthy infants aged ≤14 days were randomly assigned to either a control formula (CTRL; $n = 117$, partially hydrolyzed 100% whey-based formula) or an experimental formula (SYN; $n = 119$, CTRL supplemented with 1.77g/L of 6 HMOs [2′FL, DFL, 3FL, LNT, 3′SL, 6′SL] and *B. infantis* plus *B. lactis;* Table S1). Exclusively breastfed infants to 4 months of age were enrolled as a non-randomized reference arm (BF; $n = 82$). The primary and key secondary objectives, reported separately through age 4 months, showed that SYN supported healthy, infant-type growth, good gastrointestinal tolerance, and the expansion of beneficial bifidobacteria.[20] Blood samples were collected on a voluntary basis from CTRL ($n = 39$), SYN ($n = 35$), and BF ($n = 16$, reference) infants at 4 months of age (Figure 1A). The baseline demographics in this sub-cohort, including age, sex, weight, length, head circumference, delivery mode and number of siblings were comparable between experimental groups, indicating that randomization was maintained (Table S2). Peripheral blood mononuclear cells were isolated from venous blood and stained using a pre-validated 17-plex biomarker panel for immune cell profiling. Chip Cytometry, allowing for high-quality imaging and advanced image analyses, was used to quantify the relative abundance of 29 immune cell populations in the blood of CTRL, SYN, and BF infants. At 4 months of age, following a pattern observed in BF, the relative abundance of Th2 cells is significantly decreased in SYN compared with CTRL ($p = 0.033$, Figure 1B). For Th17 and Tregs, we observe a similar pattern with lower abundances in BF and SYN not reaching statistical significance, while Th1 cell abundance was similar between all feeding groups (Figure 1B). The relative abundance of the other 25 assessed immune cell populations is not statistically different between SYN and CTRL (Figure S1).

Next, we conducted correlation analyses to investigate a potential association between gut barrier integrity-related biomarkers and microbiome characteristics measured at 3 months of age and the observed abundances of T cell subsets (Th1, Th2, Th17, and Treg) at 4 months of age (prospective immune phenotype analyses). To this end, we focused on the biomarkers calprotectin and alpha-1-antitrypsin (AAT), measured key short-chain fatty acids ([SCFAs] acetate, propionate, butyrate), as well as bacterial taxa that were significantly different between the two randomized feeding groups CTRL and SYN in this subcohort (Figure 2). Consistent with the more balanced Th2 and Th17 states in SYN, synbiotic supplementation results in a significant reduction of the intestinal barrier biomarker AAT in SYN relative to CTRL ($p = 0.046$). This reduction follows a pattern observed in the BF reference group (Figure 2A), which was also observed in the complete trial.[20] No significant differences are observed for the intestinal inflammatory biomarker calprotectin or the concentration of acetate, propionate, and butyrate in the two randomized feeding groups (Figures 2A and 2B).

Next, we conducted correlation analyses to assess the relationships between fecal metabolites, fecal biomarkers, gut microbial taxa, and systemic T cell subsets (Figure 2C). Correlations are shown for all randomized formula-fed infants combined (CTRL + SYN) to capture global immune-microbial and immune-metabolite relationships and subsequently stratified by CTRL



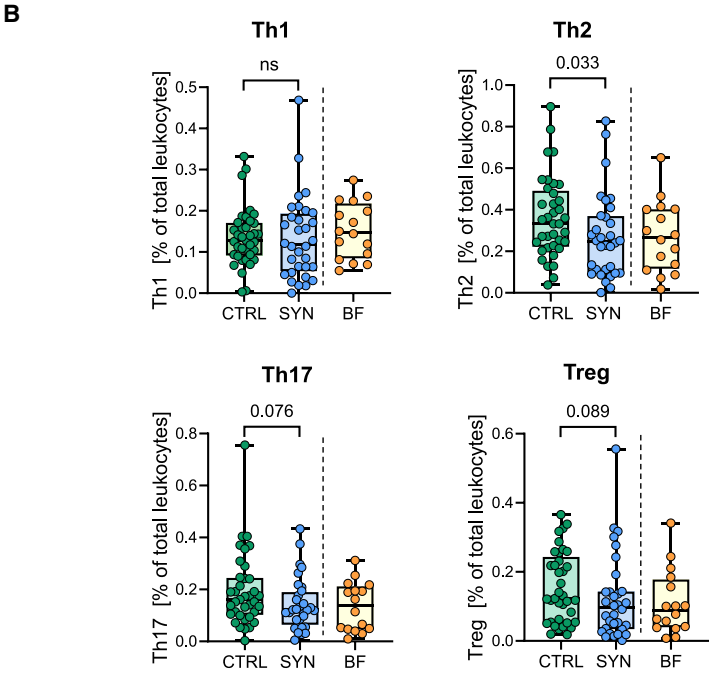


Figure 1. Early-life synbiotic supplementation silences systemic abundance of Th2 cells in formula-fed infants

(A) Schematic of the CLARA sub-cohort study protocol for blood sampling and immunotyping at 4 months.

(B) Frequencies of Th1, Th2, Th17, and Treg cells illustrated as the percentage of total blood leukocytes in CTRL, SYN, and BF infants at 4 months of age. Data are represented as box and whiskers plots illustrating median, quartiles (boxes), and range (whiskers). Statistical testing between CTRL and SYN was performed using non-parametric Mann-Whitney U test. The dotted line separates the values of non-randomized BF (used as the reference group) from randomized CTRL and SYN groups.

and SYN to assess group-specific associations. When stratified by feeding group, correlation analyses reveal distinct SCFA-immune association patterns between CTRL and SYN. In CTRL infants, butyrate and propionate show predominantly negative correlations (blue) with T cell subsets, reaching nominal significance for Th2 cells and extending to Th17 cells and Tregs, with propionate showing false discovery rate (FDR)-adjusted negative association with Tregs. In contrast, SYN-supplemented infants display a reoriented and more coordinated pattern, with SCFAs showing positive correlations (red) across assessed T cell subsets; notably, acetate is positively associated with Th2 cells at nominal significance. A divergent pattern is also observed for calprotectin, which is negatively associated with Th2 and Th17 cells (FDR significant) and Tregs (nominal) in CTRL infants, but shows positive associations (red) with T cell subsets in SYN. Together, these findings indicate that SYN supplementation may strengthen the functional coupling between microbial-derived SCFAs and systemic T cell responses.

Th1, Th2, Th17, and Treg cells are positively associated (red) with *B. infantis* abundance in SYN-supplemented infants, reaching nominal significance for Th1 cells and FDR-adjusted significance for Tregs. Further, the opportunistic pathobionts *Rothia*, *Peptoniphilus C,* Peptococcales, Mycobacteriales, and Erysipelotrichales exhibit significantly higher changes in abundance in CTRL compared with SYN. In contrast, *Enterococcus D gallinarum*, *Parabacteroides merdeae*, *UMGS1071sp900542375*, and *Blautia A wexleraea*, which have a significantly higher abundance in SYN compared with CTRL, exhibit a negative correlation (blue) with Th2 cells. Among the latter, the next-generation probiotic candidate *B. wexlerae* was previously identified to play a protective role from later allergies.[21] *Parabacteroides merdae* was additionally identified to be causally related to atopic dermatitis using Mendelian randomization.[22] *Gemella haemolysans B* and *Streptococcus thermophilus,* both with a significantly higher abundance in SYN compared with CTRL, positively correlate with Th subsets. Further, *S. thermophilus*, reported to have strong immunomodulatory and anti-allergenic properties,[23] displays a nominally significant positive correlation with Th2 cells (Figure 2C).

To further explore the interactions between immune cell subsets, we used Spearman correlation matrices to identify modules of differentially regulated immune cell populations in the blood of the two randomized feeding groups CTRL and SYN. In these analyses, we find positive correlations of Th1 cells with Th2, Th17, Treg cells, and $CD38^+$ plasmablasts (short-lived antibody-producing cells) in SYN, but not CTRL, infants (Figure S2). Conversely, in CTRL, but not SYN, naive $CD4^+$ T cells negatively correlate with naive $CD8^+$ T cells and central memory, effector memory, and effector $CD4^+$ and $CD8^+$ T cells. Together, these findings show that early-life supplementation with SYN can

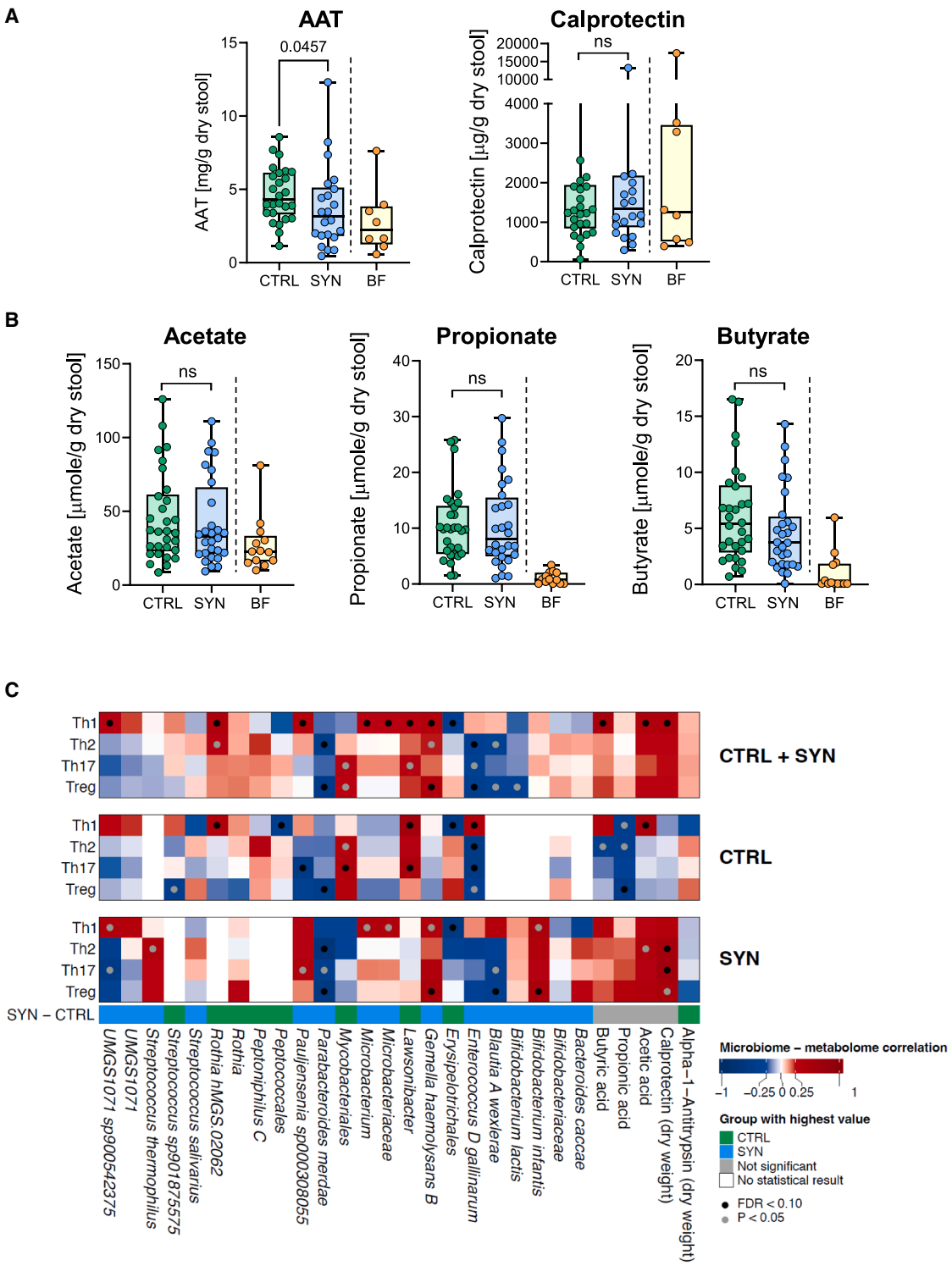


Figure 2. Effect of early-life synbiotic supplementation on fecal biomarkers of gut health, organic acids, and microbiome-metabolome-immune correlations

(A) Alpha-1-antitrypsin (AAT) and calprotectin levels in feces of CTRL, SYN, and BF infants at 3 months of age.

(B) Quantification of acetate, propionate, and butyrate in the feces of CTRL, SYN, and BF infants at 3 months of age.

(C) Heatmaps showing Spearman correlation coefficients between selected gut microbial taxa, fecal metabolites, and inflammatory biomarkers with systemic T cell subsets (Th1, Th2, Th17, and Treg) measured in infant peripheral blood.

(legend continued on next page)

shape systemic immune signatures in healthy formula-fed infants, including reduced Th2 abundance and coordinated immune regulatory networks that may be linked to beneficial immune development.

SYN supplementation ameliorates LRI severity in a neonatal mouse model of respiratory infection

Although a long-term follow-up of infants for immune-related outcomes in the randomized controlled trial would be valuable, the small sample size, high dropout rates over time, and various confounding factors (e.g., dietary influences and antibiotic exposures) prohibited this. To overcome these limitations, we employed a high-fidelity preclinical model that controls for genetics, diet, and microbial and environmental exposures, enabling us to functionally validate potential short- and long-term health benefits of clinically observed synbiotic-driven immune modulation in early life. To simulate the human epidemiology associating sLRI in early life with increased risk of later-life chronic respiratory disease,[24,25] we employed an established model of neonatal viral airway infection that increases susceptibility to allergic airway inflammation in later life.[26,27] Using a maternal low-fiber diet (LFD) setting that predisposes to sLRI via distortion of the microbiota and perturbed immune maturation in the offspring,[27] thereby mimicking a real-world risk trajectory, neonatal mice reared to LFD-fed mothers were supplemented with either a synbiotic (SYN), consisting of *B. infantis* (LMG11588) and the 6HMO clinical mix, or its individual components, namely, 6HMOs (PRE) or *B. infantis* (PRO) from postnatal day (PND) 5 to PND 20 (Figure 3A). At PND 10, mice were inoculated with pneumonia virus of mice ([PVM], murine respiratory syncytial virus homolog) to assess LRI severity. Importantly, maternal LFD feeding did not alter the weight of pregnant mothers or neonates (hereafter referred to as ''LFD-reared neonates'') at birth comparable to controls fed a high-fiber diet ([HFD], data not shown). In response to PVM infection, and compared with control HFD-reared neonates, LFD-reared neonates present with stunted weight gain, indicative of severe disease (Figure 3B). At 10 days post-infection (dpi), when the hallmark pathologies of sLRI peak,[26–28] airway epithelial sloughing, mucus hypersecretion, and airway smooth muscle remodeling are significantly elevated in PVM-infected LFD-reared neonates compared with HFD controls (Figures 3C–3E; Figures S3A–S3C). Strikingly, SYN supplementation is sufficient to lower infection-induced growth stunting and decreased the hallmark pathologies of sLRI in susceptible LFD-reared neonates (Figures 3B–3E; Figures S3A–S3C). In contrast, PRE or PRO were without effect. At 5 dpi, the peak of infection in this model, SYN supplementation prevents the loss of viral control that develops in LFD-reared neonates,[27] whereas PRE or PRO had no effect (Figure 3F). At 10 dpi, viral protein was undetectable in all groups (data not shown), consistent with our previous observations relating to the kinetics of viral clearance.[27] Taken together, these results demonstrate that early-life supplementation with an infant-type synbiotic reduces LRI severity in susceptible neonates, with SYN supplementation showing superior efficacy compared with PRE or PRO supplementation alone.

Our previous studies have demonstrated that maternal LFD feeding predisposes to sLRI in the offspring due to the delayed expansion of pDCs and Treg cells in the lungs.[26,27] To assess whether the observed increase in disease tolerance in SYN-supplemented LFD-reared neonates correlated with a restoration of pDCs and Treg cells at 5 dpi and the prevention of an overzealous immune response at 10 dpi, the lungs and mediastinal lymph nodes (MLNs) of the control and biotic supplementation groups (PRE, PRO, and SYN) were excised and immune cells quantified (gating strategy shown in Figures S4A and S4B). In line with reduced morbidity (Figures 3B–3F), early-life SYN supplementation restores the compromised pDC and Treg cell numbers in both the lungs (Figures 3G and 3H) and MLNs (Figures S5A and S5B) of LFD-reared mice at 5 dpi. Similar trends are observed for conventional DC1 (cDC1) and cDC2 numbers, particularly in the MLNs (Figures S5C–S5F). As we previously observed an association between DC hematopoiesis and expression of the non-redundant DC-active growth factor Fms-like tyrosine kinase 3 ligand (Flt3L) in the gut,[27] we next measured Flt3L concentrations in response to biotic supplementation. SYN, but not PRE or PRO, supplementation led to a significant increase of Flt3L protein concentrations in the small intestine (Figure 3I), consistent with the restoration of DC hematopoiesis.

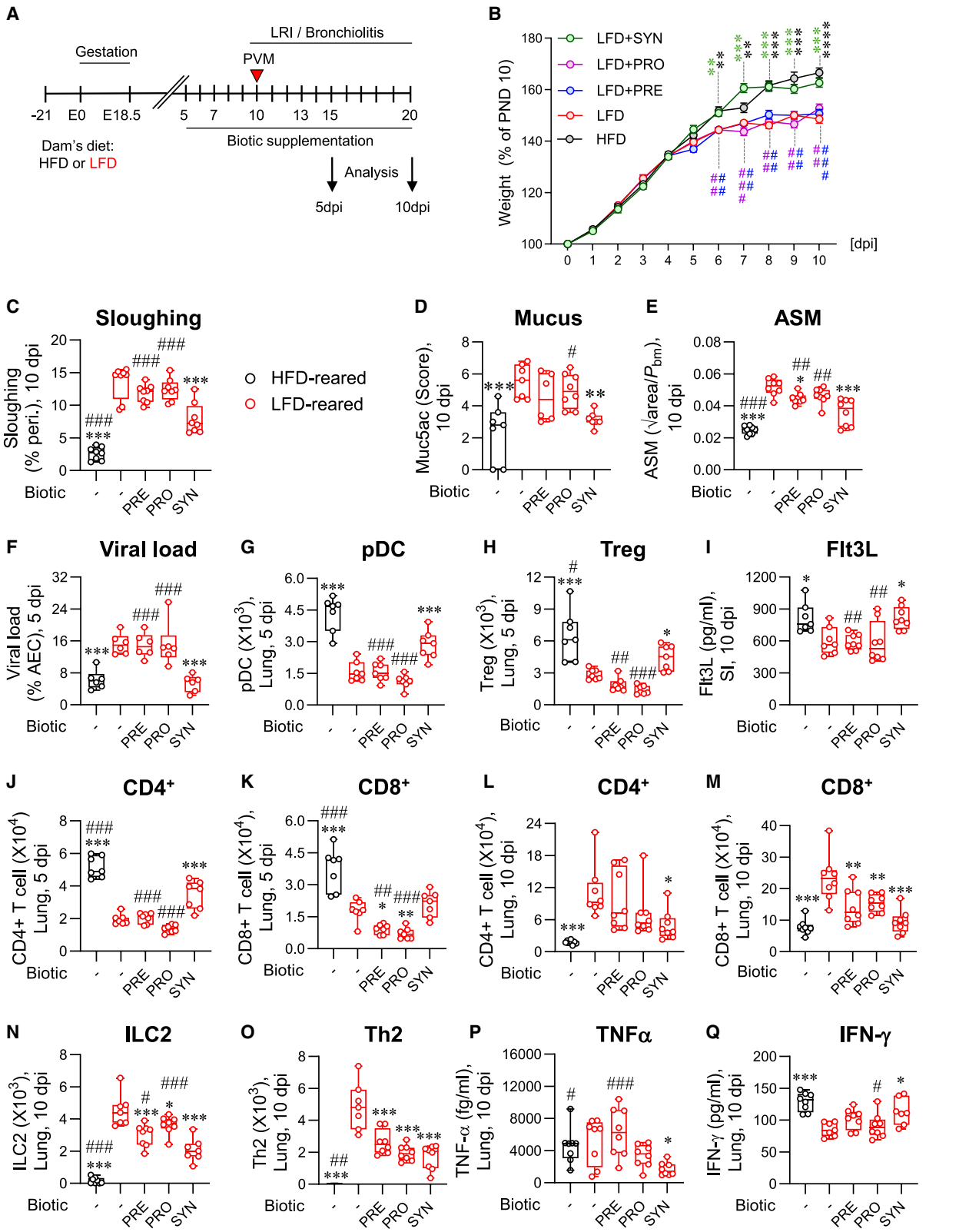
Supplementation with SYN, but not PRE or PRO, induces a significant increase in $CD4^+$, but not $CD8^+$ T cells in the lungs of LFD-reared mice at 5 dpi (Figures 3J and 3K), while both $CD4^+$ and $CD8^+$ T cells are significantly elevated in the MLNs (Figures S5G and S5H). In the absence of a timely and controlled expansion of immune cells at the peak of infection, the host response to PVM becomes over-exuberant, and it is this excessive inflammation and consequent immunopathology, despite the absence of detectable virus, that causes disease morbidity.[26,27] In line with this, at 10 dpi, the numbers of $CD4^+$ and $CD8^+$ T cells (Figure 3L and 3M), as well as pDCs, Treg cells, and cDC1 and cDC2 cells (Figures S6A–S6D) are significantly lower in the lungs of SYN-supplemented neonates compared with the susceptible control LFD-reared neonates, with similar findings in the MLNs (Figures S6E–S6J).

sLRIs can initiate aberrant Th2-driven inflammation, with longitudinal studies revealing that heightened type-2 inflammation in infants hospitalized with viral LRIs have an increased risk of developing asthma in later stages of life.[29] At 10 dpi, the numbers of $CD4^+$ Th2 cells and type-2 innate lymphoid cells (ILC2), key cellular drivers of type-2 inflammation, are significantly higher

Data are shown for all randomized formula-fed infants pooled (CTRL + SYN, top) to visualize overall immune-metabolite and immune-microbial associations across the cohort, followed by stratified analyses for CTRL (middle) and SYN (bottom) groups to assess group-specific patterns. Red and blue indicate positive and negative correlations, respectively. Dots denote statistical significance: black dots indicate correlations significant after false discovery rate (FDR) correction (FDR <0.10), and gray dots indicate nominal significance ($p < 0.05$). Correlations were assessed using Spearman rank tests.

Data in (A and B) are represented as box and whiskers plots illustrating median, quartiles (boxes), and range (whiskers).

Statistical testing between CTRL and SYN was performed using non-parametric Mann-Whitney U test. The dotted line separates the non-randomized BF reference group (not included in statistical testing) from the randomized CTRL and SYN groups.



(legend on next page)

in the lungs and MLNs of LFD- compared with HFD-reared neonates (Figures 3N and 3O; Figures S6K and S6L). Early-life SYN supplementation decreases both cell populations and elicits a superior effect relative to PRE or PRO supplementation on ILC2 numbers, but not Th2 cells. SYN supplementation is further associated with reduced TNFα and increased IFN-γ protein levels at 10 dpi in the lungs, reflecting changes in the inflammatory milieu (Figures 3P and 3Q). Collectively, these findings indicate that supplementation with an infant-type synbiotic alters the kinetics of the immune response in susceptible mice to more closely align with that observed in protected controls. While PRE and PRO elicit measurable effects on select cellular and histological parameters, SYN shows the most consistent improvements on clinically and pathologically meaningful outcomes, including reduced viral burden at the peak of infection, restoration of immunoregulatory pDCs and Tregs, and a marked decrease in morbidity and immunopathology.

Synbiotic supplementation alters gut microbiota composition and circulating metabolome correlating with improved infection outcomes

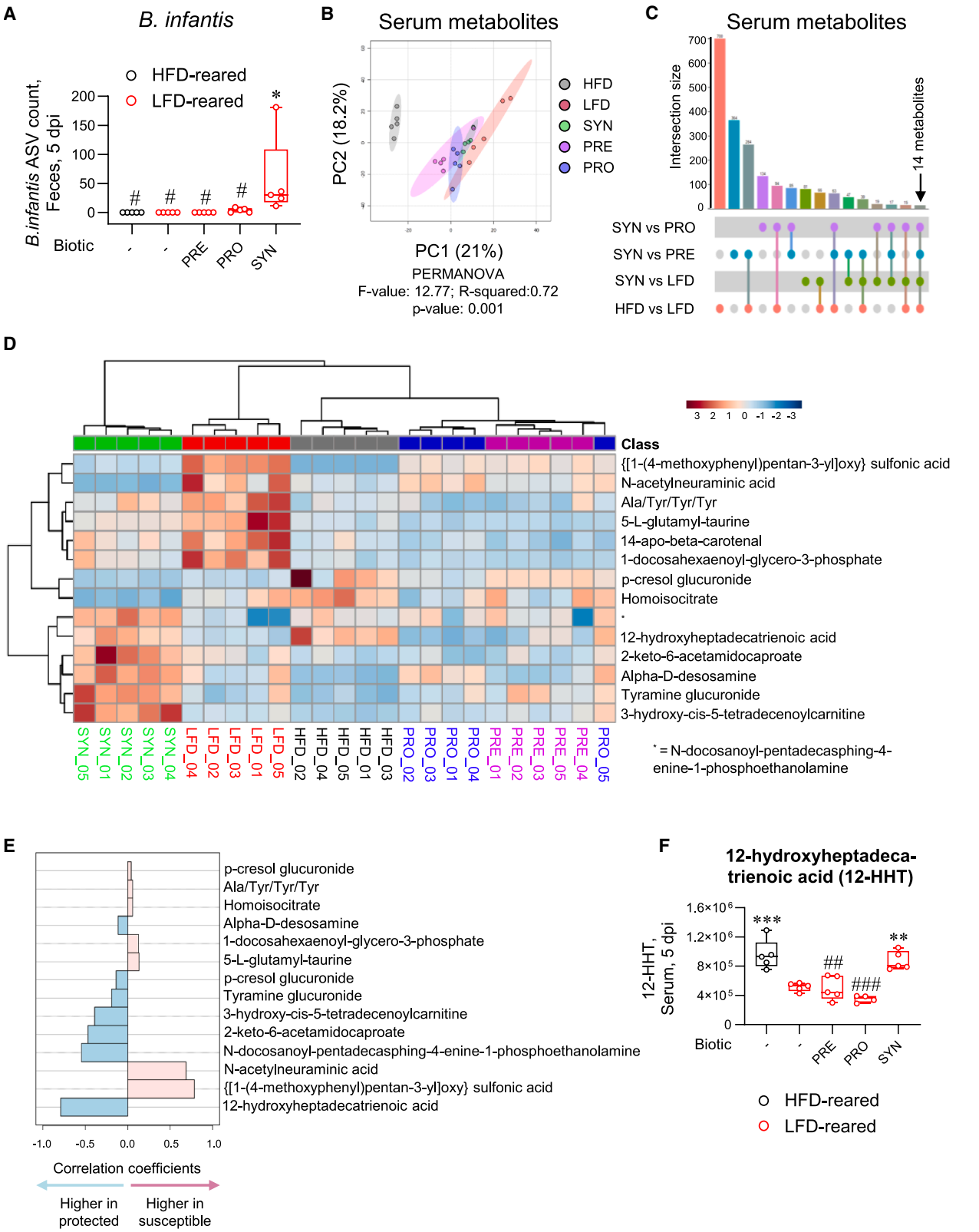
We have previously demonstrated that the increased sLRI susceptibility of LFD-reared neonates is associated with a perturbed gut microbiome and metabolome.[27] Therefore, we investigated whether SYN supplementation to susceptible LFD-reared neonates alters the gut microbiome and metabolite profiles toward HFD-reared protected controls. To do so, we profiled the fecal microbiota and serum metabolites in PVM-infected neonates and assessed the compositional changes in response to SYN, PRE, or PRO at the peak of infection (5 dpi). Alpha diversity metrics for richness (observed features), evenness (Pielou's evenness), or Shannon's entropy are not affected by SYN supplementation (Figures S7A–S7C). Fecal microbiota composition evaluated by beta diversity (weighted UniFrac distance) of LFD-reared neonates is different compared with HFD-reared controls but unaffected by biotic supplementations (Figure S7D). To address fecal microbiota compositional changes in the susceptible groups in response to biotic supplementations, we next performed pairwise comparisons (Figures S7E–S7H). In these comparisons, *B. infantis* is significantly enriched in SYN, but not the PRE and PRO supplementation groups (Figure 4A). Because *B. infantis* occurred at very low relative abundance in fecal samples, making proportional values misleading, we reported amplicon sequence variant counts as they more accurately capture biologically meaningful, probiotic engraftment relevant to infection outcomes. The enhanced abundance of *B. infantis* upon SYN, but not PRO, supplementation is in line with previous reports highlighting the reliance of *B. infantis* on HMOs for engraftment.[30,31] Further, SYN supplementation leads to the enrichment of several bacterial taxa including *Lawsonibacter sp000492175* (Figures S7F–S7H), a member of the *Lawsonibacter* genus, which have been previously shown to be depleted in patients with respiratory infections.[32,33]

To assess the changes in metabolic profiles linked to different biotic supplementations (PRE, PRO, and SYN), we performed liquid chromatography-mass spectrometry (LC-MS) on the serum of PVM-infected neonates at 5 dpi, given the influx of protective pDCs and Treg cells has been initiated in protected mice by this time. Similar to the fecal microbiota profile, the global blood metabolome of LFD-reared neonates clustered differently from HFD-reared neonates and overlapped with LFD-reared animals supplemented with PRE, PRO, or SYN (Figure 4B). Among 1,142 putative compounds in an untargeted metabolomics screen, 611 metabolites are differentially abundant between HFD- and LFD-reared neonates (Figure 4C; Figure S8A). As SYN supplementation provided superior protection against PVM infection relative to PRE or PRO supplementation alone (i.e., reversing body weight stunting, decreasing viral load, and restoring pDC and Tregs), we conducted further investigations by associating the metabolites with sLRI (i.e., protection or susceptibility). Using Metaboanalyst 6.0,[34] we constructed an UpSet plot to identify a subset of metabolites showing consistent

Figure 3. SYN supplementation ameliorates LRI severity in a neonatal mouse model of respiratory infection

(A) Study design.
(B) Weight gain during PVM infection.
(C) Sloughing of airway epithelium.
(D) Goblet cell hyperplasia and airway intraluminal mucus plugging (Muc5ac).
(E) Airway smooth muscle (ASM) thickness.
(F) Viral load in lung epithelial cells at 5 dpi.
(G) pDCs in lungs at 5 dpi.
(H) Treg cells in lungs at 5 dpi.
(I) Flt3L protein levels in small intestine (SI) at 10 dpi.
(J) $CD4^+$ T cell numbers in lungs at 5 dpi.
(K) $CD8^+$ T cell numbers in lungs at 5 dpi.
(L) $CD4^+$ T cell numbers in lungs at 10 dpi.
(M) $CD8^+$ T cell numbers in lungs at 10 dpi.
(N) ILC2 cell numbers in lungs at 10 dpi.
(O) Th2 cell numbers in lungs at 10 dpi.
(P) TNFα protein levels in lung tissues at 10 dpi.
(Q) IFN-γ protein levels in lung tissues at 10 dpi.

HFD-reared neonates represented by bars or circles outlined in black; LFD-reared neonates represented by bars or circles outlined in red. Data (n = 7–8 mice per group) represented as mean ± SEM or box and whiskers (median, quartiles, and range), p values ($^*p < 0.05$, $^{**}p < 0.01$, and $^{***}p < 0.001$ when compared with LFD-reared neonates; $^{\#}p < 0.05$, $^{\#\#}p < 0.01$, and $^{\#\#\#}p < 0.001$ when compared with SYN-supplemented neonates) were derived from one-way ANOVA followed by Dunnett's multiple test (C–Q) or two-way ANOVA followed by Tukey's multiple comparison test (B). Pairwise comparisons for all groups are summarized in Table S4.



(legend on next page)

directional differences across comparisons between groups classified as phenotypically protected (HFD-reared neonates and SYN-supplemented LFD-reared neonates) and phenotypically susceptible (LFD-reared neonates and PRE- or PRO-supplemented LFD-reared neonates; Figure 4C). A total of 14 metabolites met these criteria and are highlighted for further association analyses. A heatmap of these 14 metabolites showed tight intra-group clustering (Figure 4D). Among the 7 metabolites that were associated with protection (Figure 4E), 12-hydroxyheptadecatrienoic acid (12-HHT) and N-docos anoyl-pentadecasphing-4-enine-1-phosphoethanolamine significantly correlate with protection from sLRI ($p < 0.05$, Figures S8B and S8C). Of note, the peak intensity of the highest ranked metabolite 12-HHT is significantly higher in the protected compared with the susceptible groups and significantly higher in SYN relative to PRE- or PRO-supplemented neonates (Figure 4F). Conversely, the metabolites {[1-(4-methoxyphenyl) pentan-3-yl]oxy}sulfonic acid and N-acetyl-a-neuraminic acid are more abundant in the susceptible groups, and SYN supplementation is sufficient to significantly decrease the levels of these putative disease-associated metabolites (Figures S8D–S8F). Collectively, our findings indicate that SYN supplementation is associated with selective effects on specific gut microbial taxa and systemic metabolites, with protection against sLRIs linked to defined metabolite features rather than global alterations of the gut microbiome.

SYN supplementation in early life decreases later-life susceptibility to pollution-enhanced allergic airway inflammation

Epidemiological studies have demonstrated that sLRIs in early life are a major independent risk factor for the later development of asthma.[13,24,35–37] To mimic such a scenario, we exposed previously PVM-infected mice to an allergic sensitization protocol in the presence of particulate matter (PM2.5), an environmental pollutant known for its ability to induce asthma exacerbations.[38–40] LFD-reared neonates were infected with PVM (PND 10) prior to sensitization with cockroach allergen extract (CRE) in the presence of PM2.5 starting at PND 42 (PM-CRE experimental asthma, Figure 5A). Remarkably, SYN supplementation, restricted to the neonatal period, confers lasting protection against the subsequent development of allergic airway inflammation. Specifically, we observe a significant reduction in infiltrating eosinophils and classical and SiglecF+ neutrophils to the lungs of mice supplemented with SYN in early life compared with controls (Figures 5B and 5C; Figures S9A and S9B) that is paralleled by reduced airway smooth muscle remodeling (Figures 5D and 5E). Consistent with the curtailed granulocytic inflammation, the type-2 cellular response (i.e., ILC2 and Th2 cells) and associated mucus hypersecretion are significantly ameliorated in the lungs of adult mice that had been supplemented with SYN in early life (Figures 5F–5I). In line with the observed synergistic effect of 6HMOs together with *B. infantis* in reducing LRI severity (Figures 3C–3E), the protective effect of SYN on pollution-enhanced allergic airway inflammation is more pronounced than that observed with PRE or PRO supplementation (Figure 5; Figure S9). In summary, our findings indicate that early-life SYN supplementation markedly decreases the severity of sLRIs and associated type-2 inflammation in early life and has long-lasting beneficial effects that persist into adulthood, even in the absence of continued SYN supplementation.

SYN supplementation in early life alters select gut microbial taxa and systemic metabolome in later life

To test whether the protective effects of SYN on later-life development of allergic airway inflammation were associated with specific gut microbial signatures and metabolite profiles in adulthood, we profiled fecal samples for microbiota structure and the sera for metabolites at PND 66 (the age at which asthma-like pathologies were assessed). The fecal microbiota composition of HFD-reared neonates shows distinct clustering compared with LFD-reared neonates and was structurally different in adulthood (PND 66; Figures S10A–S10E). However, early-life biotic supplementations (PRE, PRO, or SYN) do not induce significant changes to either alpha or beta diversity in adulthood (Figures S10A–S10D). In line with the cessation of SYN supplementation at weaning, the increased *B. infantis* abundance in early life (Figure 4A) does not persist into adulthood, similar to clinical observations where *B. infantis* colonizes the infant gut but is typically absent in adults.[31] Pairwise comparisons revealed that LFD-reared neonates supplemented with SYN in early life exhibit lower abundance of *Romboutsia ilealis* in adulthood but are enriched for *Sporofaciens sp910574885* and *NM07-P-09 sp012584445* when compared with untreated or PRO supplemented mice (Figures S10F and S10G). Susceptible groups (LFD—reared neonates and PRE- and PRO-supplemented LFD-reared neonates) consistently exhibit a lower abundance of *Sporofaciens sp910574885* compared with the protected groups (HFD-reared neonates and SYN-supplemented LFD-reared pups; Figures S10F–S10H). Moreover, the

Figure 4. Synbiotic supplementation alters gut microbiota composition and circulating metabolome correlating with improved infection outcomes

(A) Amplicon sequence variant (ASV) counts of *B. infantis* in feces at 5 dpi.

(B) Principal-component analysis (PCA) illustrates serum metabolic profiles of the various groups at 5 dpi.

(C) UpSet diagram illustrates differences in serum metabolite levels in each set of comparisons at 5 dpi. Colored bars represent inter-group comparisons between 2 or more groups. Set numbers denote the number of differentially abundant serum metabolites common to each set of comparisons.

(D) Heatmap of 14 differentially regulated serum metabolites common to each set of comparisons. Heatmap colors indicate log-fold changes.

(E) Correlation analysis of serum metabolites associated with protection or susceptibility.

(F) Peak intensity of 12-HHT (12-hydroxyheptadecatrienoic acid) at 5 dpi.

Data (n = 7–8 mice per group) represented as box and whiskers plot illustrating median, quartiles (boxes), and range (whiskers). HFD-reared neonates represented by bars outlined in black; LFD-reared neonates represented by bars outlined in red.

p values ($^{*}p < 0.05$, $^{**}p < 0.01$, and $^{***}p < 0.001$ when compared with LFD-reared neonates; $^{\#}p < 0.05$, $^{\#\#}p < 0.01$, and $^{\#\#\#}p < 0.001$ when compared with SYN-supplemented neonates) were derived from one-way ANOVA followed by Dunnett's multiple test.

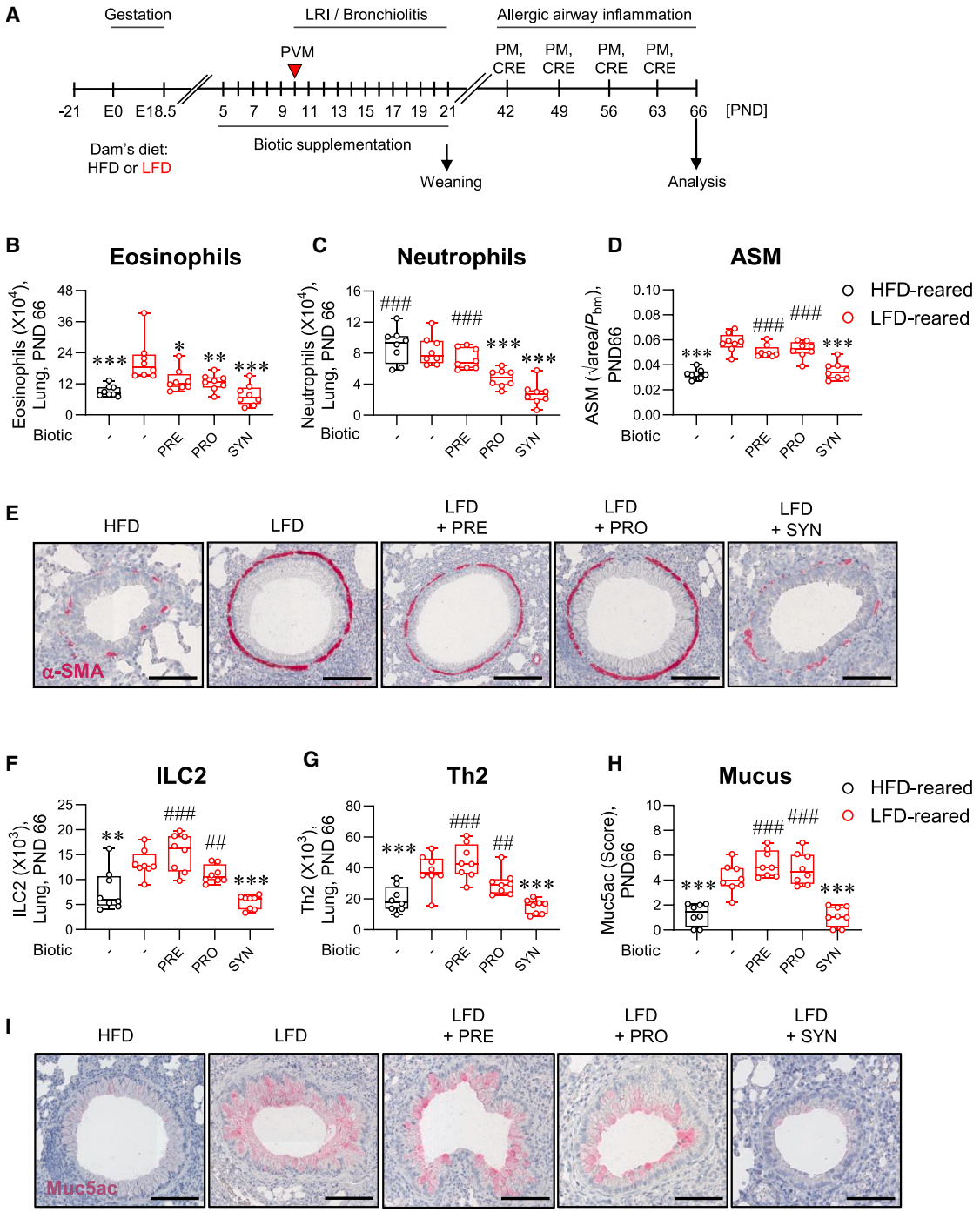


Figure 5. SYN supplementation in early life decreases later-life susceptibility to pollution-enhanced allergic airway inflammation

(A) Study design.

(B) Eosinophil numbers in lungs at PND 66.

(C) Neutrophil numbers in lungs at PND 66.

(D) Airway smooth muscle (ASM) thickness at PND 66.

(E) Representative micrographs (×20) of airway smooth muscles (red, α-SMA) at PND 66; scale bars, 100 μm.

(F) ILC2 cell numbers in lungs at PND 66.

(G) Th2 cell numbers in lungs at PND 66.

(H) Goblet cell hyperplasia and airway intraluminal mucus plugging (Muc5ac) in lungs at PND 66.

(I) Representative micrographs (×20) of airway intraluminal mucus plugging (pink, Muc5a) at PND 66; scale bars, 100 μm.

(legend continued on next page)

abundance of *Akkermansia muciniphila* is greater in HFD- compared with LFD-reared mice, and SYN supplementation of LFD-reared neonates in early life increases the abundance of *Akkermansia muciniphila* in adulthood (Figures S10E and S10F), which is noteworthy as this taxon is associated with resistance against the development of childhood asthma.[41]

Akin to our findings at PND15, early-life SYN supplementation alters the profile of circulating metabolites at PND66 (Figure 6A; Figure S11B). Strikingly, SYN-supplemented mice cluster separately from susceptible controls and PRE-supplemented and PRO-supplemented LFD-reared neonates, even though the nutritional supplementation had ceased for greater than 6 weeks (Figure 6A; Figure S11B). Metaboanalyst 6.0[34] was used to perform downstream analysis of serum metabolomic profile obtained from LC-MS. Of the 1,135 metabolites measured, the mean intensity of 480 metabolites differed significantly between groups (Figure S11A). The UpSet plot, constructed by comparing the protected groups (HFD-reared pups, SYN) with the susceptible groups, identified 175 metabolites with directional differences across comparisons (Figure 6B). Metabolites were then ranked based on correlation coefficients by the ''Pattern Search'' function in Metaboanalyst 6.0. Of the top 25 metabolites, 22 are associated with protection against and 3 metabolites are linked with predisposition to asthma-like disease in later life (Figures 6C and 6D; Figures S11C and S11D). Strikingly, while SYN-treated mice display a distinct global metabolic profile, SYN supplementation shifts the levels of a subset of metabolites toward those observed in protected controls (Figure 6C; Figure S11B). The metabolites 2,5-dimethyl-3-furanthiol acetate and amino caproic acid are most highly correlated with protection against disease (Figure 6D; Figure S11C), with both being elevated in HFD-reared mice and susceptible LFD-reared mice supplemented with SYN (Figures 6E and 6F). In contrast, indicine,{3-[2-(3-hydroxy-5-methoxyphenyl) ethyl] phenyl} oxidanesulfonic acid and N(6)-methyllysine positively associate with susceptibility to allergic airway inflammation, with high concentrations observed in LFD-reared controls and those supplemented with PRE or PRO alone (Figure 6C; Figure S11D). Together, our findings suggest that SYN supplementation in early life modulates specific gut microbial taxa (rather than broad ecosystem wide changes) and circulating metabolite profiles in later life. Whether these SYN supplementation-associated durable effects are associative or causal in protecting against later-life susceptibility and progression to chronic experimental asthma remains to be determined.

12-HHT supplementation in early life confers protection against sLRI

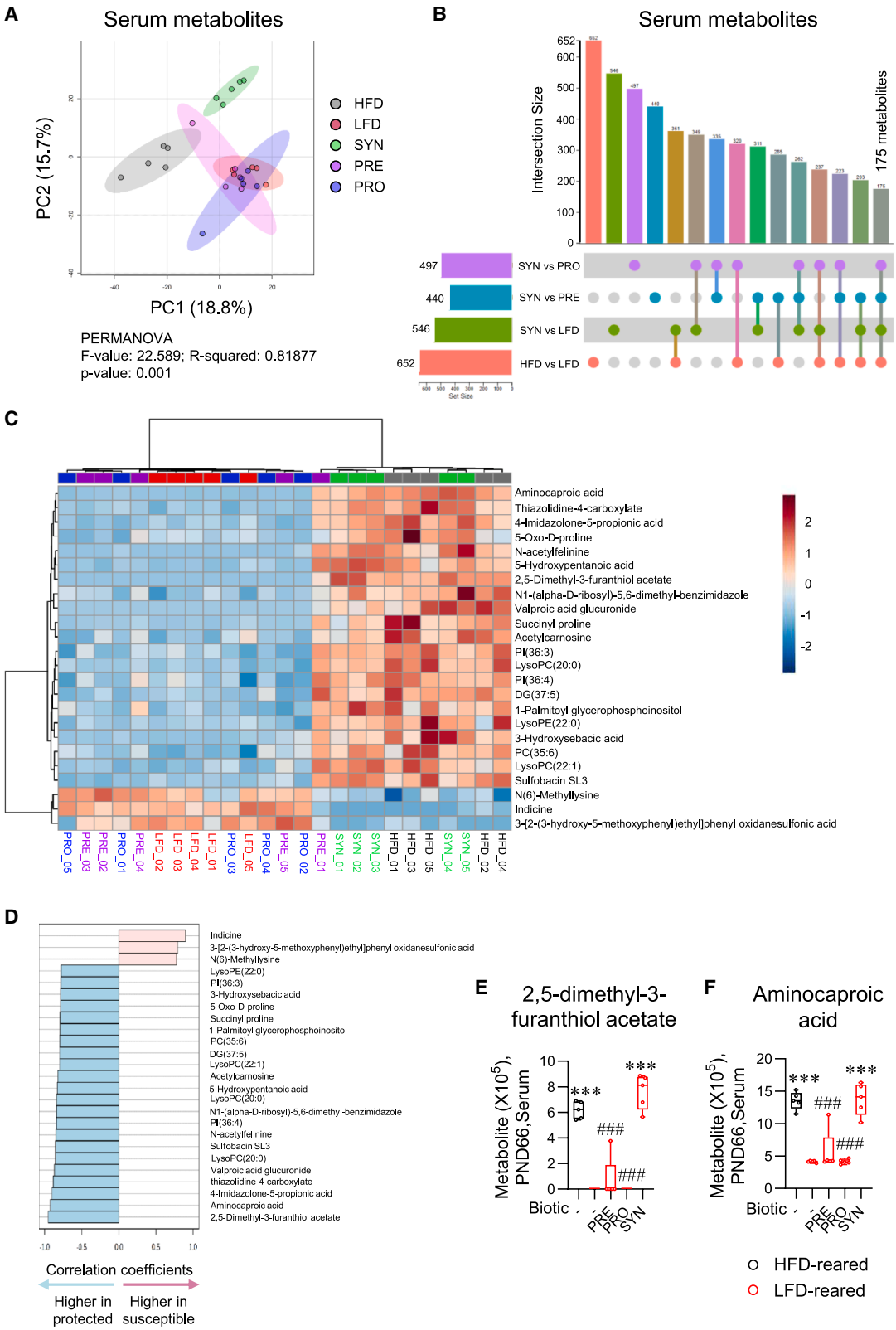
To determine whether the metabolite 12-HHT—identified through synbiotic-associated systemic metabolomic signatures (Figure 4)—plays a causal role in protecting against the development of an sLRI, we performed *in vivo* 12-HHT supplementation studies in neonatal mice inoculated with PVM (Figure 7A). Strikingly, oral administration of 12-HHT to LFD-reared neonates is sufficient to prevent infection-induced growth stunting and the development of airway remodeling and tissue damage in the lungs at 10 dpi (Figures 7B–7E). At the peak of infection (5 dpi), the viral load is lower, and lung pDC and Treg numbers are higher, in neonates supplemented with 12-HHT (Figures 7F–7H). Notably, the restoration in pDC is associated with the increased expression of Flt3L in the small intestine (Figure 7I). Consistent with improved clinical outcomes, and rescue of the pDC-Treg-associated immunoregulatory axis, the T cell immune response at 5 and 10 dpi in 12-HHT-supplemented neonates broadly follows the pattern observed in protected controls (Figures 7J–7N). Together, these findings causally link a metabolite elevated in synbiotic-protected neonates, 12-HHT, to improved infection outcomes by demonstrating that targeted metabolite supplementation can recapitulate key phenotypic and immunologic benefits of the synbiotic intervention.

DISCUSSION

Modulating states of microbial imbalance in early life via supplementation with prebiotics, probiotics, or combinations thereof (synbiotics) is increasingly pursued to support immune development and long-term health. Extending previous work on infant-type bifidobacteria, we show that supplementation with an infant-type synbiotic, previously shown to be safe, well tolerated, and an augmenter of beneficial infant-type bifidobacteria,[20] promotes coordinated SCFA-linked metabolite-immune interactions and attenuates a Th2 bias, aligning with patterns observed in exclusively breastfed infants. Using reverse-translational, infant-relevant infection and environmental challenge models, early-life synbiotic supplementation through weaning enhances immune resilience by improving disease tolerance to LRIs in early life and reduces later susceptibility to pollution-enhanced allergic airway disease. Together, these data support a model in which early-life synbiotic exposure shapes baseline metabolite-immune interactions, priming the developing immune system for improved resilience to future challenges, an aspect that cannot be directly tested in healthy infants and was, therefore, addressed in complementary preclinical models.

For newborns to thrive, the development of the immune system must be balanced, yet proceed at a rapid but controlled pace shortly after birth to adapt to changing environmental challenges. Unlike adults, neonates exhibit Th2-skewed immune profiles that enable organ development and survival of the fetus by minimizing the potential for maternal-fetal allogenic reactions.[42–44] As a trade-off, newborns have a T cell system that is reduced in Th1 capacity, which is necessary to mount an effective anti-viral defense.[45–47] Alterations in the dynamics of immune system adaptation in early life are associated with increased susceptibility to lower respiratory illnesses in early

Data (n = 7–8 mice per group) represented as box and whiskers plot illustrating median, quartiles (boxes), and range (whiskers).
HFD-reared neonates represented by bars outlined in black; LFD-reared neonates represented by bars outlined in red.
p values (*$p < 0.05$, **$p < 0.01$, and ***$p < 0.001$ when compared with LFD-reared neonates; $^{\#\#}p < 0.01$, and $^{\#\#\#}p < 0.001$ when compared with SYN-supplemented neonates) were derived from one-way ANOVA followed by Dunnett's multiple test. Pairwise comparisons for all groups are summarized in Table S4.



(legend on next page)

childhood, which in turn, represent an independent risk factor for the subsequent development of persistent asthma later in life.[48] Our findings in this randomized, multicenter design study conducted across several European sites demonstrate that synbiotic supplementation in early life is sufficient to reduce a sustained systemic Th2 bias and unbalanced Th17 cell abundance at 4 months of age, following a pattern observed in breastfed infants. These findings are in line with a previous report demonstrating that low abundance of bifidobacterial species and/or lack of HMO-utilization capacity in breastfed infants is associated with enteric inflammation, driven by aberrant Th2 and Th17 responses.[6] Given Th2 abundance in early life has been identified as a risk factor for the development of chronic inflammatory disorders later in life,[49–51] rationally designed, infant-type biotics may help to prevent or mitigate unfavorable immune imprinting in early life manifesting in long-term health outcomes.

In response to synbiotic supplementation, we identify modules of differentially regulated immune cell populations in SYN, but not CTRL, formula-fed infants. We hypothesize that early-life SYN supplementation may promote a more balanced immune development and/or activation states. In line with this hypothesis, SYN supplementation enhances a functional coupling between Treg and effector T cells (Th1, Th2, and Th17) compared with CTRL infants, suggesting a more balanced response between activation and immunoregulation. Conversely, significant negative correlations between naive $CD4^+$ T cells and effector and memory T cell subsets are observed in CTRL- but not SYN-supplemented infants. Thus, SYN supplementation may stabilize and strengthen immune cell interactions, even without necessarily altering the absolute frequencies of these cells. Additional investigations employing systems immunology approaches, which encompass longitudinal assessments of cellular abundance, activation states, and effector molecule capacity, will contribute to a more comprehensive understanding of synbiotic-driven changes in systemic immune signatures and immune system development rates in early life.

Despite the reported changes in systemic immune profiles with SYN supplementation, we did not observe significant changes in parent-reported physician-confirmed adverse events between SYN, CTRL, and BF healthy infants at 4 months of age (data not shown). While previous studies have associated *B. infantis* colonization in early life with decreased risk of enteric virus infections and atopic diseases within the first 2 years of age,[18,52] continued examination of this study cohort and follow-up health questionnaires will offer a longitudinal perspective on the potential health outcomes associated with early-life synbiotic supplementation. While this study was conducted in healthy, term infants, synbiotic intervention to promote long-term health may have a more pronounced effect in at-risk individuals, such as infants with a family history of atopy or those exposed to nutritional imbalances during pregnancy.

A strength of this study is the inclusion of infant-relevant disease models, which not only enable functional testing of hypotheses generated in the clinical SYN supplementation trial but also demonstrates efficacy in promoting disease tolerance. Using a clinically relevant setup of maternal LFD feeding to increase infection risk in the offspring,[27,53] we demonstrate that early-life synbiotic supplementation is sufficient to reverse compromised immune programs including sustained Th2 immune responses upon viral infection in preclinical models that control for genetics, diet, and environmental exposures. In these settings, synbiotic supplementation, but not individual supplementation of PRE or PRO, confers protection against sLRI in early life and pollution-enhanced allergic airway inflammation later in life. These findings further emphasize the importance of developing infant-type synbiotics to maximize the health benefits driven by prebiotics and probiotics.

Timely and regulated activation of different T cells by DCs is a critical factor for determining the outcome of respiratory infections.[27,54] Our findings demonstrate that early-life synbiotic supplementation is sufficient to restore a compromised pDC-Treg axis in the lungs and draining lymph nodes of susceptible LFD-reared neonatal mice, previously shown to be necessary and sufficient for bronchiolitis disease management.[26] Although SYN supplementation expanded pDCs and Tregs, additional studies are required to establish whether this immunoregulatory axis is causally responsible for observed immune protection in this setting. Consistent with preclinical findings, Konieczna et al. demonstrated that *B. infantis* supplementation stimulated pDC-mediated $Foxp3^+$ Treg responses in the peripheral blood of healthy adult volunteers.[55] These findings provide further evidence that *B. infantis* supplementation may have the potential to induce coordinated pDC-Treg responses to support improved infection outcomes via the induction of disease tolerance. While we cannot rule out other mechanisms contributing to pDC and Treg expansion, we demonstrate that synbiotic supplementation significantly increases intestinal levels of Flt3L—a cytokine essential for pDC development—providing a plausible mechanistic link by which an oral synbiotic may enhance immune responses at distal mucosal sites such as the lung.

Remarkably, we find that synbiotic-mediated immune benefits persisted throughout adolescence, even though synbiotic

Figure 6. SYN supplementation in early life alters the gut microbiome and systemic metabolome in later life

(A) PCA illustrates the serum metabolic profiles of the various groups at PND 66.

(B) UpSet diagram illustrating differences in serum metabolite levels in each set of comparisons at PND 66. Set numbers denote the number of differentially abundant metabolites common to each set of comparisons.

(C) Correlation analysis of serum metabolites associated with protection or susceptibility.

(D) Heatmap of differentially regulated serum metabolites common to each set of comparisons. Heatmap colors indicate log-fold changes. Heatmap of serum metabolites associated with protection and susceptibility.

(E and F) (E) Peak intensity of 2,5-dimethyl-3-furanthiol acetate and (F) aminocaproic acid at PND 66.

Data (n = 7–8 mice per group) represented as box and whiskers plot illustrating median, quartiles (boxes), and range (whiskers). HFD-reared neonates represented by bars outlined in black; LFD-reared neonates represented by bars outlined in red.

p values ($^*p < 0.05$, $^{**}p < 0.01$, and $^{***}p < 0.001$ when compared with LFD-reared neonates; $^{\#}p < 0.05$, $^{\#\#}p < 0.01$, and $^{\#\#\#}p < 0.001$ when compared with SYN-supplemented neonates) were derived from one-way ANOVA followed by Dunnett's multiple test.

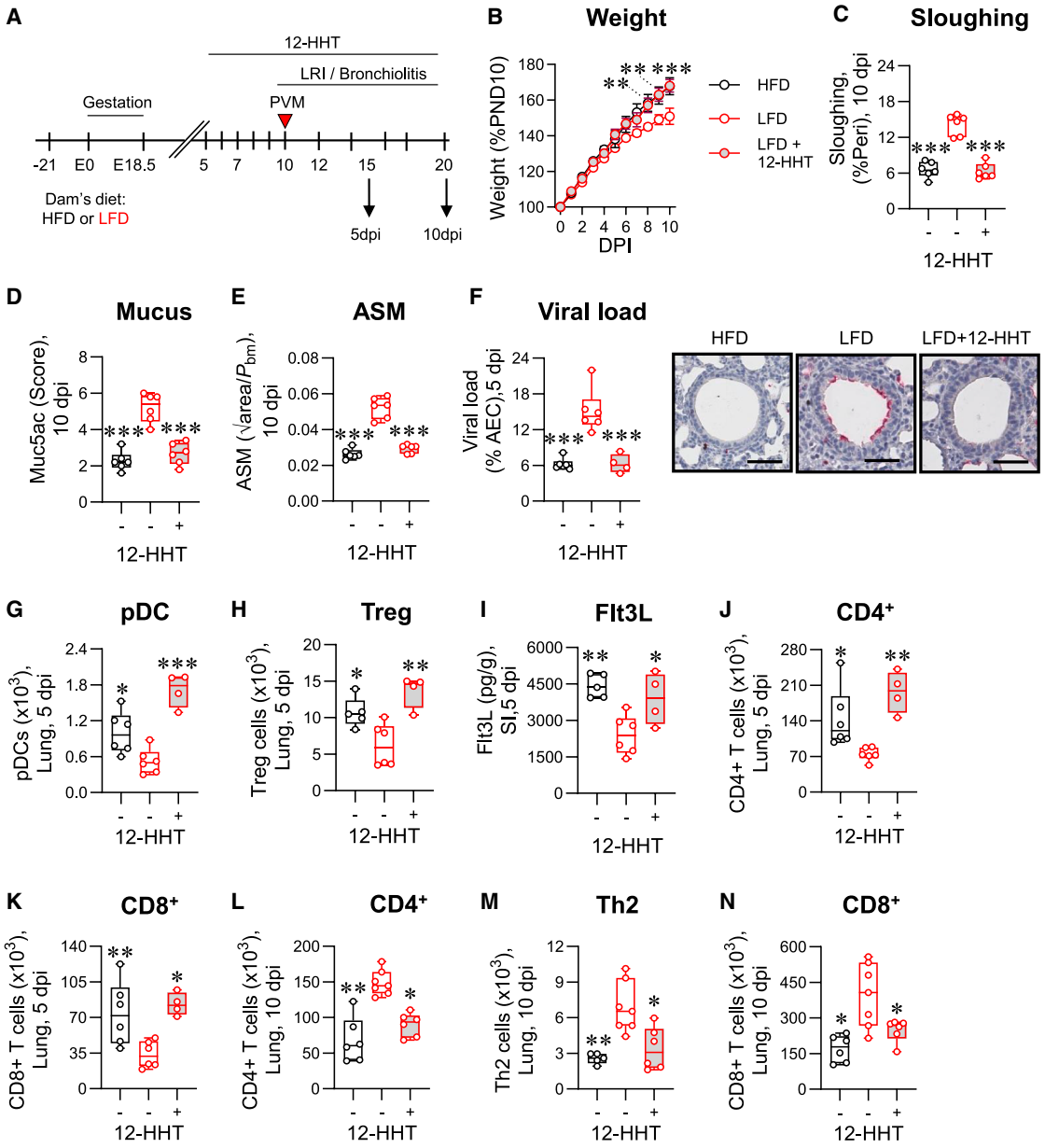


Figure 7. 12-HHT supplementation in early life confers protection against sLRI

(A) Study design.
(B) Weight gain during PVM infection.
(C) Sloughing of airway epithelium.
(D) Goblet cell hyperplasia and airway intraluminal mucus plugging (Muc5ac).
(E) Airway smooth muscle (ASM) thickness.
(F) Viral load in airway epithelial cells at 5 dpi and representative micrographs (×20) of PVM immunoreactivity (red) in the airway epithelium at 5 dpi. Scale bars, 100 μm.
(G) pDC in lungs at 5 dpi.
(H) Treg cells in lungs at 5 dpi.
(I) Flt3L protein levels in small intestine (SI) at 5 dpi.
(J) $CD4^+$ T cell numbers in lungs at 5 dpi.
(K) $CD8^+$ T cell numbers in lungs at 5 dpi.
(L) $CD4^+$ T cell numbers in lungs at 10 dpi.
(M) Th2 cell numbers in lungs at 10 dpi.
(N) $CD8^+$ T cell numbers in lungs at 10 dpi.

(legend continued on next page)

supplementation was discontinued at weaning. In line with our preclinical findings, Dai et al. previously reported that breastfeeding enrichment of *B. infantis* is associated with reduced antibiotic-associated asthma risk in children, with *B. infantis* abundance positively correlating with fucosylated HMOs in paired maternal samples.[56] Further research is required to resolve whether the improved disease tolerance upon synbiotic supplementation in the preclinical model is attributable to early-life immune system imprinting, the prevention of aberrant tissue remodeling following an sLRI, or a combination of both.

A central contribution of this study is the integration of systemic metabolomics, revealing that synbiotic supplementation in the context of a viral infection induces broad systemic metabolic remodeling, including enrichment of metabolites associated with disease protection. Among these, the lipid mediator 12-HHT emerged as a host-microbial effector linking early-life microbial states to improved infection outcomes.12-HHT has been previously implicated in epithelial repair, inflammation resolution, and lipid mediator signaling, but its role in early-life antiviral immunity has not been fully elucidated. Engagement of 12-HHT with its cognate receptor, Blt2 (leukotriene B4 receptor 2), which is expressed by epithelial and immune cells, results in downstream production of cytokines, chemokines, and matrix metalloproteinases, which can calibrate an over-exuberant immune response and limit the potential for immunopathology following infection.[57–60] The involvement of 12-HHT in promoting wound healing[58,61,62] and the fact that BLT2-deficient mice are more susceptible to acute lung injury[63] and eosinophilic lung inflammation[63] further emphasize a potential beneficial role of 12-HHT in regulating immune responses and promoting tissue repair. Our study results indicate that 12-HHT is not merely correlated with protection from sLRI, it is causally sufficient. Oral supplementation with 12-HHT phenocopies the protective effects of synbiotic supplementation, preventing infection-induced growth stunting, reducing viral burden, promoting pDC and Treg responses, and calibrating the immune response to limit immunopathology and disease severity. These findings underscore the concept that host-derived lipid mediators may act as key effector molecules linking early-life microbial states to immunological resilience. Indeed, 12-HHT increased Flt3L expression in the gut, which we have previously linked to neonatal hematopoiesis of DCs, which serve as the immune system's key decision makers.[27] By establishing 12-HHT as a functional mediator of disease tolerance, our findings bridge observational metabolomics with functional outcomes and support a model in which early-life host-microbial interactions shape the host lipid mediator landscape to tune immune responsiveness. Further studies are needed to delineate the cellular sources and regulatory pathways governing 12-HHT production in early life, its receptor-mediated mechanisms across tissues, and its therapeutic potential in human populations at high risk for viral or allergic diseases.

Among other metabolites that were significantly associated with higher disease susceptibility were {[1-(4-methoxyphenyl)-pentan-3-yl]oxy}sulfonic acid and N-acetyl-a-neuraminic acid, with the latter being involved in virus adherence to host cells and regulating viral replication.[64,65] In line with its potential role as a systemic biomarker of inflammation, N-acetyl-a-neuraminic acid serum levels are significantly reduced in SYN- compared with LFD-reared control, PRE-, or PRO-supplemented groups.

Early-life synbiotic supplementation also leads to persistent effects on the systemic metabolome later in life, with several of these metabolites associated with protection or susceptibility to experimental asthma. Among the two metabolites with the highest correlation coefficients for protection are 2,5-dimethyl-3′-formylthiazole and aminocaproic acid, while only 3 metabolites are associated with negative outcomes. Thiazole derivates such as 2,5-dimethyl-3′-formylthiazole are known for their anti-inflammatory and antioxidant effects,[66] while aminocaproic acid has anti-fibrinolytic properties.[67] Whether observed alterations in circulating metabolites in later life directly contribute to the protective effect of early-life SYN supplementation on preventing the development of pollution-enhanced allergic airway inflammation or are biomarkers of a healthy immune system and microbiome remains to be determined.

Collectively, these data provide a comprehensive and multidimensional view on the important role of an infant-type synbiotic in imprinting the immune system to promote health in early life with potential long-term effects. More broadly, they advance the conceptual framework that targeted modulation of host-metabolic networks can tune early-life immune trajectories and promote durable immune health. Given the critical role of early-life nutrition in shaping healthy microbiome and immune trajectories, integrating rationally designed, infant-type synbiotic solutions during key windows of immunological development may present a practical alternative when breastfeeding is not an option.

Limitations of the study

Limitations of this study include (1) the relatively small sample size for infant blood immunotyping and single time-point analysis, (2) limited statistical power to link reduced Th2 abundance with clinical outcomes at 4 months, and (3) numerical (non-significant) imbalance in mode of delivery. Continued cohort follow-up and health questionnaires may provide longitudinal insight into early-life infant-type synbiotic-driven immune imprinting, which is currently best examined using complementary preclinical models that do not fully recapitulate healthy human infant physiology.

RESOURCE AVAILABILITY

Lead contact

Further information and requests for resources and reagents should be directed to and will be fulfilled by the lead contact, Simon Phipps (simon.phipps@qimrb.edu.au).

HFD-reared neonates represented by bars or circles outlined in black; LFD-reared neonates represented by bars or circles outlined in red. Data (n = 7–8 mice per group) represented as mean ± SEM or box and whiskers (median, quartiles, and range), p values (*$p < 0.05$, **$p < 0.01$, and ***$p < 0.001$ when compared with LFD-reared neonates; $^{\#}p < 0.05$, $^{\#\#}p < 0.01$, and $^{\#\#\#}p < 0.001$ when compared with SYN-supplemented neonates) were derived from one-way ANOVA followed by Dunnett's multiple test (C–N) or two-way ANOVA followed by Tukey's multiple comparison test (B).

Materials availability

This study did not generate new unique reagents.

Data and code availability

Mouse sequencing data generated in this study have been deposited in the European Nucleotide Archive (ENA) under accession number ENA: PRJEB113220. Mouse metabolome data have been deposited at https://zenodo.org/records/20184749. Summary-level data supporting human findings are provided within the manuscript and its supplemental information (Table S5). Raw sequencing data are protected and not publicly available due to pediatric patient privacy concerns (risk of re-identification from individual sequencing data, even without direct identifiers). Access to these data may be considered on a case-by-case basis for non-commercial research purposes, subject to review of the proposed research objectives to ensure compliance with GDPR guidelines. The requester must describe the objectives of the research project and enter into a data access agreement in accordance with applicable data protection requirements. To ensure patient privacy, access to personally identifiable information or sensitive clinical information will not be provided, and any data access must strictly comply with the consent conditions agreed with study participants. This paper does not report original code. All analyses were performed using R (RStudio) with publicly available, well-established R packages and did not involve novel algorithms or non-standard analytical workflows. Any additional information required to reanalyze the mouse data reported in this work paper is available from the lead contact upon request.

CONSORTIA

The members of the CLARA study group are Olivier Claris, Mercedes Gil-Campos, Ignacio Salamanca De La Cueva, Luc Cornette, Philippe Alliet, André Léké, Mireille Castanet, Hugues Piloquet, Virginie de Halleux, Delphine Mitanchez, Yvan Vandenplas, Pierre Maton, Frank Jochum, Dirk Olbertz, Sergio Negre Policarpo, and Javier Miranda-Mallea.

ACKNOWLEDGMENTS

We extend our sincere gratitude to the parents and caregivers who generously consented to their infants' participation and to the study teams across all institutions for their exemplary efforts in study organization and conduct. We thank Tristan Bourdeau for preparation and coordination of ingredient shipment to QIMR and Colin Cercamondi for assistance in clinical trial design. We thank Dr. Martha Zakrzewski at the Australian Genome Research Facility for performing the 16S long-read analysis. Graphical abstract was generated with BioRender.com.

AUTHOR CONTRIBUTIONS

J.C.P., N.S., S.P. and M.N. designed the research; R.B.R., C.K.C., T.A., CLARA study group, D.R.H., P.N., I.S., T.W., M.S.R., J.P.M., D.J.C., J.M.M., K.V., C.F., D.M., N.P.H., E.F.-B., and I.S.-Z. conducted the research; R.B.R., L.L., and J.M.M. analyzed the data; R.B.R., S.P., and M.N. wrote the manuscript. All authors read and approved the final manuscript.

DECLARATION OF INTERESTS

C.K.C., K.V., C.F., L.L., D.M., N.P.H., I.S.-Z., E.F.-B., N.S., and M.N. are employees of Société des Produits Nestlé S.A. (SPN), the sponsor of this trial. J.-C.P. and CLARA Study Group members received a grant from SPN to conduct clinical study. R.B.R., T.A., T.W., M.S.R., P.N., I.S., D.R.H., and S.P. are employees of the QIMR Berghofer MRI, with whom SPN had a collaboration agreement to conduct pre-clinical studies. J.M.M. is an employee of Cmbio, with whom SPN had a service agreement. The investigational products were provided by S.P.N. E.F.B., D.M., and M.N. have filed patent applications related to combinations of HMOs and *B. infantis* (WO 2024/236049 A1, WO 2024/236050A1, and WO 2022/161865 A1).

STAR★METHODS

Detailed methods are provided in the online version of this paper and include the following:

- KEY RESOURCES TABLE
- EXPERIMENTAL MODEL AND STUDY PARTICIPANT DETAILS
  - Study design and population
  - Animal model of viral sLRI and pollution enhanced allergic airway inflammation
  - Ethics and consent to participate
- METHOD DETAILS
  - Intervention and study product
  - Adverse events and medication use
  - Fecal bifidobacterium abundance in infants
  - Human blood sampling and immunotyping analyses
  - Human fecal alpha-1-antitrypsin, calprotectin and SCFAs measurements
  - Flow cytometry mouse studies
  - Histology and immunohistochemistry mouse studies
  - Long read 16S rRNA sequencing and microbiome profiling in mice
  - Untargeted metabolic profiling in mouse samples
- QUANTIFICATION AND STATISTICAL ANALYSIS
  - Statistical analysis of human data
  - Statistical analysis of mouse data

SUPPLEMENTAL INFORMATION

Supplemental information can be found online at https://doi.org/10.1016/j.xcrm.2026.102935.

Received: August 6, 2025
Revised: April 10, 2026
Accepted: June 26, 2026
Published: July 31, 2026

REFERENCES

1. Basha, S., Surendran, N., and Pichichero, M. (2014). Immune responses in neonates. Expert Rev. Clin. Immunol. *10*, 1171–1184. https://doi.org/10.1586/1744666X.2014.942288.
2. PrabhuDas, M., Adkins, B., Gans, H., King, C., Levy, O., Ramilo, O., and Siegrist, C.A. (2011). Challenges in infant immunity: implications for responses to infection and vaccines. Nat. Immunol. *12*, 189–194. https://doi.org/10.1038/ni0311-189.
3. Torow, N., Hand, T.W., and Hornef, M.W. (2023). Programmed and environmental determinants driving neonatal mucosal immune development. Immunity *56*, 485–499. https://doi.org/10.1016/j.immuni.2023.02.013.
4. Al Nabhani, Z., and Eberl, G. (2020). Imprinting of the immune system by the microbiota early in life. Mucosal Immunol. *13*, 183–189. https://doi.org/10.1038/s41385-020-0257-y.
5. Hornef, M.W., and Torow, N. (2020). 'Layered immunity and the 'neonatal window of opportunity' - timed succession of non-redundant phases to establish mucosal host-microbial homeostasis after birth. Immunology *159*, 15–25. https://doi.org/10.1111/imm.13149.
6. Henrick, B.M., Rodriguez, L., Lakshmikanth, T., Pou, C., Henckel, E., Arzoomand, A., Olin, A., Wang, J., Mikes, J., Tan, Z., et al. (2021). Bifidobacteria-mediated immune system imprinting early in life. Cell *184*, 3884–3898.e11. https://doi.org/10.1016/j.cell.2021.05.030.
7. Ojima, M.N., Jiang, L., Arzamasov, A.A., Yoshida, K., Odamaki, T., Xiao, J., Nakajima, A., Kitaoka, M., Hirose, J., Urashima, T., et al. (2022). Priority effects shape the structure of infant-type Bifidobacterium communities on human milk oligosaccharides. ISME J. *16*, 2265–2279. https://doi.org/10.1038/s41396-022-01270-3.

8. Hickman, B., Salonen, A., Ponsero, A.J., Jokela, R., Kolho, K.L., de Vos, W.M., and Korpela, K. (2024). Gut microbiota wellbeing index predicts overall health in a cohort of 1000 infants. Nat. Commun. *15*, 8323. https://doi.org/10.1038/s41467-024-52561-6.

9. Arrieta, M.C., Arévalo, A., Stiemsma, L., Dimitriu, P., Chico, M.E., Loor, S., Vaca, M., Boutin, R.C.T., Morien, E., Jin, M., et al. (2018). Associations between infant fungal and bacterial dysbiosis and childhood atopic wheeze in a nonindustrialized setting. J. Allergy Clin. Immunol. *142*, 424–434.e10. https://doi.org/10.1016/j.jaci.2017.08.041.

10. Cox, L.M., Yamanishi, S., Sohn, J., Alekseyenko, A.V., Leung, J.M., Cho, I., Kim, S.G., Li, H., Gao, Z., Mahana, D., et al. (2014). Altering the intestinal microbiota during a critical developmental window has lasting metabolic consequences. Cell *158*, 705–721. https://doi.org/10.1016/j.cell.2014.05.052.

11. Garcia-Mauriño, C., Shao, Y., Miltz, A., Lawley, T.D., Rodger, A., and Field, N. (2025). Investigation of associations between the neonatal gut microbiota and severe viral lower respiratory tract infections in the first 2 years of life: a birth cohort study with metagenomics. Lancet Microbe *6*, 101072. https://doi.org/10.1016/j.lanmic.2024.101072.

12. Deshmukh, H., Whitsett, J., Zacharias, W., Way, S.S., Martinez, F.D., Mizgerd, J., Pryhuber, G., Ambalavanan, N., Bacharier, L., Natarajan, A., et al. (2025). Impact of Viral Lower Respiratory Tract Infection (LRTI) in Early Childhood (0-2 Years) on Lung Growth and Development and Lifelong Trajectories of Pulmonary Health: A National Institutes of Health (NIH) Workshop Summary. Pediatr. Pulmonol. *60*, e27357. https://doi.org/10.1002/ppul.27357.

13. Zar, H.J., Cacho, F., Kootbodien, T., Mejias, A., Ortiz, J.R., Stein, R.T., and Hartert, T.V. (2024). Early-life respiratory syncytial virus disease and long-term respiratory health. Lancet Respir. Med. *12*, 810–821. https://doi.org/10.1016/S2213-2600(24)00246-7.

14. Lawson, M.A.E., O'Neill, I.J., Kujawska, M., Gowrinadh Javvadi, S., Wijeyesekera, A., Flegg, Z., Chalklen, L., and Hall, L.J. (2020). Breast milk-derived human milk oligosaccharides promote Bifidobacterium interactions within a single ecosystem. ISME J. *14*, 635–648. https://doi.org/10.1038/s41396-019-0553-2.

15. Sprenger, N., Tytgat, H.L.P., Binia, A., Austin, S., and Singhal, A. (2022). Biology of human milk oligosaccharides: From basic science to clinical evidence. J. Hum. Nutr. Diet. *35*, 280–299. https://doi.org/10.1111/jhn.12990.

16. De Bruyn, F., James, K., Cottenet, G., Dominick, M., and Katja, J. (2024). Combining Bifidobacterium longum subsp. infantis and human milk oligosaccharides synergistically increases short chain fatty acid production ex vivo. Commun. Biol. *7*, 943. https://doi.org/10.1038/s42003-024-06628-1.

17. Laursen, M.F., Pekmez, C.T., Larsson, M.W., Lind, M.V., Yonemitsu, C., Larnkjær, A., Mølgaard, C., Bode, L., Dragsted, L.O., Michaelsen, K.F., et al. (2021). Maternal milk microbiota and oligosaccharides contribute to the infant gut microbiota assembly. ISME Commun. *1*, 21. https://doi.org/10.1038/s43705-021-00021-3.

18. Seppo, A.E., Bu, K., Jumabaeva, M., Thakar, J., Choudhury, R.A., Yonemitsu, C., Bode, L., Martina, C.A., Allen, M., Tamburini, S., et al. (2021). Infant gut microbiome is enriched with Bifidobacterium longum ssp. infantis in Old Order Mennonites with traditional farming lifestyle. Allergy *76*, 3489–3503. https://doi.org/10.1111/all.14877.

19. Capeding, M.R.Z., Phee, L.C.M., Ming, C., Noti, M., Vidal, K., Le Carrou, G., Frézal, A., Moll, J.M., Vogt, J.K., Myers, P.N., et al. (2023). Safety, efficacy, and impact on gut microbial ecology of a Bifidobacterium longum subspecies infantis LMG11588 supplementation in healthy term infants: a randomized, double-blind, controlled trial in the Philippines. Front. Nutr. *10*, 1319873. https://doi.org/10.3389/fnut.2023.1319873.

20. Picaud, J.C., Claris, O., Gil-Campos, M., De La Cueva, I.S., Cornette, L., Alliet, P., Léké, A., Castanet, M., Piloquet, H., de Halleux, V., et al. (2025). Partially hydrolyzed, whey-based infant formula with six human milk oligosaccharides, B. infantis LMG11588, and B. lactis CNCM I-3446 is safe, well tolerated, and improves gut health: a staged analysis of a randomized trial. Front. Nutr. *12*, 1628847. https://doi.org/10.3389/fnut.2025.1628847.

21. Hoskinson, C., Dai, D.L.Y., Del Bel, K.L., Becker, A.B., Moraes, T.J., Mandhane, P.J., Finlay, B.B., Simons, E., Kozyrskyj, A.L., Azad, M.B., et al. (2023). Delayed gut microbiota maturation in the first year of life is a hallmark of pediatric allergic disease. Nat. Commun. *14*, 4785. https://doi.org/10.1038/s41467-023-40336-4.

22. Li, W., and Li, A. (2024). Exploring the causal relationship between gut microbiota and atopic dermatitis: A Mendelian randomization study. Medicine (Baltim.) *103*, e40193. https://doi.org/10.1097/MD.0000000000040193.

23. Dargahi, N., Johnson, J., and Apostolopoulos, V. (2020). Streptococcus thermophilus alters the expression of genes associated with innate and adaptive immunity in human peripheral blood mononuclear cells. PLoS One *15*, e0228531. https://doi.org/10.1371/journal.pone.0228531.

24. Rosas-Salazar, C., Chirkova, T., Gebretsadik, T., Chappell, J.D., Peebles, R.S., Jr., Dupont, W.D., Jadhao, S.J., Gergen, P.J., Anderson, L.J., and Hartert, T.V. (2023). Respiratory syncytial virus infection during infancy and asthma during childhood in the USA (INSPIRE): a population-based, prospective birth cohort study. Lancet *401*, 1669–1680. https://doi.org/10.1016/S0140-6736(23)00811-5.

25. Rosas-Salazar, C., Hasegawa, K., and Hartert, T.V. (2023). Progress in understanding whether respiratory syncytial virus infection in infancy causes asthma in childhood. J. Allergy Clin. Immunol. *152*, 866–869. https://doi.org/10.1016/j.jaci.2023.08.009.

26. Lynch, J.P., Werder, R.B., Loh, Z., Sikder, M.A.A., Curren, B., Zhang, V., Rogers, M.J., Lane, K., Simpson, J., Mazzone, S.B., et al. (2018). Plasmacytoid dendritic cells protect from viral bronchiolitis and asthma through semaphorin 4a-mediated T reg expansion. J. Exp. Med. *215*, 537–557. https://doi.org/10.1084/jem.20170298.

27. Sikder, M.A.A., Rashid, R.B., Ahmed, T., Sebina, I., Howard, D.R., Ullah, M.A., Rahman, M.M., Lynch, J.P., Curren, B., Werder, R.B., et al. (2023). Maternal diet modulates the infant microbiome and intestinal Flt3L necessary for dendritic cell development and immunity to respiratory infection. Immunity *56*, 1098–1114.e10. https://doi.org/10.1016/j.immuni.2023.03.002.

28. Loh, Z., Simpson, J., Ullah, A., Zhang, V., Gan, W.J., Lynch, J.P., Werder, R.B., Sikder, A.A., Lane, K., Sim, C.B., et al. (2020). HMGB1 amplifies ILC2-induced type-2 inflammation and airway smooth muscle remodelling. PLoS Pathog. *16*, e1008651. https://doi.org/10.1371/journal.ppat.1008651.

29. Legg, J.P., Hussain, I.R., Warner, J.A., Johnston, S.L., and Warner, J.O. (2003). Type 1 and type 2 cytokine imbalance in acute respiratory syncytial virus bronchiolitis. Am. J. Respir. Crit. Care Med. *168*, 633–639. https://doi.org/10.1164/rccm.200210-1148OC.

30. Button, J.E., Cosetta, C.M., Reens, A.L., Brooker, S.L., Rowan-Nash, A.D., Lavin, R.C., Saur, R., Zheng, S., Autran, C.A., Lee, M.L., et al. (2023). Precision modulation of dysbiotic adult microbiomes with a human-milk-derived synbiotic reshapes gut microbial composition and metabolites. Cell Host Microbe *31*, 1523–1538.e10. https://doi.org/10.1016/j.chom.2023.08.004.

31. Button, J.E., Autran, C.A., Reens, A.L., Cosetta, C.M., Smriga, S., Ericson, M., Pierce, J.V., Cook, D.N., Lee, M.L., Sun, A.K., et al. (2022). Dosing a synbiotic of human milk oligosaccharides and B. infantis leads to reversible engraftment in healthy adult microbiomes without antibiotics. Cell Host Microbe *30*, 712–725.e7. https://doi.org/10.1016/j.chom.2022.04.001.

32. Hildebrand, C.B., Lichatz, R., Pich, A., Mühlfeld, C., Woltemate, S., Vital, M., and Brandenberger, C. (2023). Short-chain fatty acids improve inflamm-aging and acute lung injury in old mice. Am. J. Physiol. Lung Cell. Mol. Physiol. *324*, L480–L492. https://doi.org/10.1152/ajplung.00296.2022.

33. Sun, Z., Song, Z.G., Liu, C., Tan, S., Lin, S., Zhu, J., Dai, F.H., Gao, J., She, J.L., Mei, Z., et al. (2022). Gut microbiome alterations and gut barrier dysfunction are associated with host immune homeostasis in COVID-19 patients. BMC Med. *20*, 24. https://doi.org/10.1186/s12916-021-02212-0.

34. Pang, Z., Lu, Y., Zhou, G., Hui, F., Xu, L., Viau, C., Spigelman, A.F., MacDonald, P.E., Wishart, D.S., Li, S., and Xia, J. (2024). MetaboAnalyst 6.0: towards a unified platform for metabolomics data processing, analysis

and interpretation. Nucleic Acids Res. *52*, W398–W406. https://doi.org/10.1093/nar/gkae253.

35. Kusel, M.M.H., de Klerk, N.H., Kebadze, T., Vohma, V., Holt, P.G., Johnston, S.L., and Sly, P.D. (2007). Early-life respiratory viral infections, atopic sensitization, and risk of subsequent development of persistent asthma. J. Allergy Clin. Immunol. *119*, 1105–1110. https://doi.org/10.1016/j.jaci.2006.12.669.

36. Stein, R.T., Sherrill, D., Morgan, W.J., Holberg, C.J., Halonen, M., Taussig, L.M., Wright, A.L., and Martinez, F.D. (1999). Respiratory syncytial virus in early life and risk of wheeze and allergy by age 13 years. Lancet *354*, 541–545. https://doi.org/10.1016/S0140-6736(98)10321-5.

37. van Meel, E.R., den Dekker, H.T., Elbert, N.J., Jansen, P.W., Moll, H.A., Reiss, I.K., de Jongste, J.C., Jaddoe, V.W.V., and Duijts, L. (2018). A population-based prospective cohort study examining the influence of early-life respiratory tract infections on school-age lung function and asthma. Thorax *73*, 167–173. https://doi.org/10.1136/thoraxjnl-2017-210149.

38. Kim, Y., Park, E.H., Ng, C.F.S., Chung, Y., Hashimoto, K., Tashiro, K., Hasunuma, H., Doi, M., Tamura, K., Moriuchi, H., et al. (2021). Respiratory function declines in children with asthma associated with chemical species of fine particulate matter (PM2.5) in Nagasaki, Japan. Environ. Health. *20*, 110. https://doi.org/10.1186/s12940-021-00796-x.

39. Murrison, L.B., Brandt, E.B., Myers, J.B., and Hershey, G.K.K. (2019). Environmental exposures and mechanisms in allergy and asthma development. J. Clin. Investig. *129*, 1504–1515. https://doi.org/10.1172/JCI124612.

40. Li, X., and Liu, X. (2021). Effects of PM2.5 on Chronic Airway Diseases: A Review of Research Progress. Atmosphere *12*, 1068.

41. Michalovich, D., Rodriguez-Perez, N., Smolinska, S., Pirozynski, M., Mayhew, D., Uddin, S., Van Horn, S., Sokolowska, M., Altunbulakli, C., Eljaszewicz, A., et al. (2019). Obesity and disease severity magnify disturbed microbiome-immune interactions in asthma patients. Nat. Commun. *10*, 5711. https://doi.org/10.1038/s41467-019-13751-9.

42. McFadden, J.P., Thyssen, J.P., Basketter, D.A., Puangpet, P., and Kimber, I. (2015). T helper cell 2 immune skewing in pregnancy/early life: chemical exposure and the development of atopic disease and allergy. Br. J. Dermatol. *172*, 584–591. https://doi.org/10.1111/bjd.13497.

43. Simon, A.K., Hollander, G.A., and McMichael, A. (2015). Evolution of the immune system in humans from infancy to old age. Proc. Biol. Sci. *282*, 20143085. https://doi.org/10.1098/rspb.2014.3085.

44. Zaghouani, H., Hoeman, C.M., and Adkins, B. (2009). Neonatal immunity: faulty T-helpers and the shortcomings of dendritic cells. Trends Immunol. *30*, 585–591. https://doi.org/10.1016/j.it.2009.09.002.

45. Crofts, K.F., and Alexander-Miller, M.A. (2020). Challenges for the Newborn Immune Response to Respiratory Virus Infection and Vaccination. Vaccines (Basel) *8*, 558. https://doi.org/10.3390/vaccines8040558.

46. Ota, M.O.C., Vekemans, J., Schlegel-Haueter, S.E., Fielding, K., Whittle, H., Lambert, P.H., McAdam, K.P.W.J., Siegrist, C.A., and Marchant, A. (2004). Hepatitis B immunisation induces higher antibody and memory Th2 responses in new-borns than in adults. Vaccine *22*, 511–519. https://doi.org/10.1016/j.vaccine.2003.07.020.

47. Vekemans, J., Ota, M.O.C., Wang, E.C.Y., Kidd, M., Borysiewicz, L.K., Whittle, H., McAdam, K.P.W.J., Morgan, G., and Marchant, A. (2002). T cell responses to vaccines in infants: defective IFNgamma production after oral polio vaccination. Clin. Exp. Immunol. *127*, 495–498. https://doi.org/10.1046/j.1365-2249.2002.01788.x.

48. Jackson, D.J., Gangnon, R.E., Evans, M.D., Roberg, K.A., Anderson, E.L., Pappas, T.E., Printz, M.C., Lee, W.M., Shult, P.A., Reisdorf, E., et al. (2008). Wheezing rhinovirus illnesses in early life predict asthma development in high-risk children. Am. J. Respir. Crit. Care Med. *178*, 667–672. https://doi.org/10.1164/rccm.200802-309OC.

49. Borbet, T.C., Pawline, M.B., Zhang, X., Wipperman, M.F., Reuter, S., Maher, T., Li, J., Iizumi, T., Gao, Z., Daniele, M., et al. (2022). Influence of the early-life gut microbiota on the immune responses to an inhaled allergen. Mucosal Immunol. *15*, 1000–1011. https://doi.org/10.1038/s41385-022-00544-5.

50. Fu, Y., Lou, H., Wang, C., Lou, W., Wang, Y., Zheng, T., and Zhang, L. (2013). T cell subsets in cord blood are influenced by maternal allergy and associated with atopic dermatitis. Pediatr. Allergy Immunol. *24*, 178–186. https://doi.org/10.1111/pai.12050.

51. Herberth, G., Daegelmann, C., Röder, S., Behrendt, H., Krämer, U., Borte, M., Heinrich, J., Herbarth, O., and Lehmann, I.; LISAplus study group (2010). IL-17E but not IL-17A is associated with allergic sensitization: results from the LISA study. Pediatr. Allergy Immunol. *21*, 1086–1090. https://doi.org/10.1111/j.1399-3038.2010.01033.x.

52. Colston, J.M., Taniuchi, M., Ahmed, T., Ferdousi, T., Kabir, F., Mduma, E., Nshama, R., Iqbal, N.T., Haque, R., Ahmed, T., et al. (2022). Intestinal Colonization With Bifidobacterium longum Subspecies Is Associated With Length at Birth, Exclusive Breastfeeding, and Decreased Risk of Enteric Virus Infections, but Not With Histo-Blood Group Antigens, Oral Vaccine Response or Later Growth in Three Birth Cohorts. Front. Pediatr. *10*, 804798. https://doi.org/10.3389/fped.2022.804798.

53. Ferolla, F.M., Hijano, D.R., Acosta, P.L., Rodríguez, A., Dueñas, K., Sancilio, A., Barboza, E., Caría, A., Gago, G.F., Almeida, R.E., et al. (2013). Macronutrients during pregnancy and life-threatening respiratory syncytial virus infections in children. Am. J. Respir. Crit. Care Med. *187*, 983–990. https://doi.org/10.1164/rccm.201301-0016OC.

54. Lynch, J.P., Werder, R.B., Curren, B.F., Sikder, M.A.A., Ullah, A., Sebina, I., Rashid, R.B., Zhang, V., Upham, J.W., Hill, G.R., et al. (2020). Long-lived regulatory T cells generated during severe bronchiolitis in infancy influence later progression to asthma. Mucosal Immunol. *13*, 652–664. https://doi.org/10.1038/s41385-020-0268-8.

55. Konieczna, P., Groeger, D., Ziegler, M., Frei, R., Ferstl, R., Shanahan, F., Quigley, E.M.M., Kiely, B., Akdis, C.A., and O'Mahony, L. (2012). Bifidobacterium infantis 35624 administration induces Foxp3 T regulatory cells in human peripheral blood: potential role for myeloid and plasmacytoid dendritic cells. Gut *61*, 354–366. https://doi.org/10.1136/gutjnl-2011-300936.

56. Dai, D.L.Y., Petersen, C., Hoskinson, C., Del Bel, K.L., Becker, A.B., Moraes, T.J., Mandhane, P.J., Finlay, B.B., Simons, E., Kozyrskyj, A.L., et al. (2023). Breastfeeding enrichment of B. longum subsp. infantis mitigates the effect of antibiotics on the microbiota and childhood asthma risk. Méd. Sur *4*, 92–112.e5. https://doi.org/10.1016/j.medj.2022.12.002.

57. Giusti, F., Casiraghi, M., Point, E., Damian, M., Rieger, J., Bon, C.L., Pozza, A., Moncoq, K., Banères, J.L., and Catoire, L.J. (2020). Structure of the agonist 12-HHT in its BLT2 receptor-bound state. Sci. Rep. *10*, 2630. https://doi.org/10.1038/s41598-020-59571-6.

58. Liu, M., Saeki, K., Matsunobu, T., Okuno, T., Koga, T., Sugimoto, Y., Yokoyama, C., Nakamizo, S., Kabashima, K., Narumiya, S., et al. (2014). 12-Hydroxyheptadecatrienoic acid promotes epidermal wound healing by accelerating keratinocyte migration via the BLT2 receptor. J. Exp. Med. *211*, 1063–1078. https://doi.org/10.1084/jem.20132063.

59. Okuno, T., and Yokomizo, T. (2018). Biological functions of 12(S)-hydroxyheptadecatrienoic acid as a ligand of leukotriene B(4) receptor 2. Inflamm. Regen. *38*, 29. https://doi.org/10.1186/s41232-018-0087-4.

60. Saeki, K., and Yokomizo, T. (2017). Identification, signaling, and functions of LTB(4) receptors. Semin. Immunol. *33*, 30–36. https://doi.org/10.1016/j.smim.2017.07.010.

61. Iizuka, Y., Okuno, T., Saeki, K., Uozaki, H., Okada, S., Misaka, T., Sato, T., Toh, H., Fukayama, M., Takeda, N., et al. (2010). Protective role of the leukotriene B4 receptor BLT2 in murine inflammatory colitis. FASEB J. *24*, 4678–4690. https://doi.org/10.1096/fj.10-165050.

62. Iwamoto, S., Koga, T., Ohba, M., Okuno, T., Koike, M., Murakami, A., Matsuda, A., and Yokomizo, T. (2017). Non-steroidal anti-inflammatory drug delays corneal wound healing by reducing production of 12-hydroxyheptadecatrienoic acid, a ligand for leukotriene B(4) receptor 2. Sci. Rep. *7*, 13267. https://doi.org/10.1038/s41598-017-13122-8.

63. Matsunaga, Y., Fukuyama, S., Okuno, T., Sasaki, F., Matsunobu, T., Asai, Y., Matsumoto, K., Saeki, K., Oike, M., Sadamura, Y., et al. (2013).

Leukotriene B4 receptor BLT2 negatively regulates allergic airway eosinophilia. FASEB J. *27*, 3306–3314. https://doi.org/10.1096/fj.12-217000.

64. Burzyńska, P., Sobala, Ł.F., Mikołajczyk, K., Jodłowska, M., and Jaśkiewicz, E. (2021). Sialic Acids as Receptors for Pathogens. Biomolecules *11*, 831. https://doi.org/10.3390/biom11060831.

65. Wasik, B.R., Barnard, K.N., and Parrish, C.R. (2016). Effects of Sialic Acid Modifications on Virus Binding and Infection. Trends Microbiol. *24*, 991–1001. https://doi.org/10.1016/j.tim.2016.07.005.

66. Farghaly, T.A., Alfaifi, G.H., and Gomha, S.M. (2024). Recent Literature on the Synthesis of Thiazole Derivatives and their Biological Activities. Mini Rev. Med. Chem. *24*, 196–251. https://doi.org/10.2174/1389557523666230726142459.

67. Garewal, H.S., and Durie, B.G. (1985). Anti-fibrinolytic therapy with aminocaproic acid for the control of bleeding in thrombocytopenic patients. Scand. J. Haematol. *35*, 497–500. https://doi.org/10.1111/j.1600-0609.1985.tb02818.x.

68. Curren, B., Ahmed, T., Howard, D.R., Ashik Ullah, M., Sebina, I., Rashid, R.B., Al Amin Sikder, M., Namubiru, P., Bissell, A., Ngo, S., et al. (2023). IL-33-induced neutrophilic inflammation and NETosis underlie rhinovirus-triggered exacerbations of asthma. Mucosal Immunol. *16*, 671–684. https://doi.org/10.1016/j.mucimm.2023.07.002.

69. Bosheva, M., Tokodi, I., Krasnow, A., Pedersen, H.K., Lukjancenko, O., Eklund, A.C., Grathwohl, D., Sprenger, N., Berger, B., and Cercamondi, C.I.; 5 HMO Study Investigator Consortium (2022). Infant Formula With a Specific Blend of Five Human Milk Oligosaccharides Drives the Gut Microbiota Development and Improves Gut Maturation Markers: A Randomized Controlled Trial. Front. Nutr. *9*, 920362. https://doi.org/10.3389/fnut.2022.920362.

70. Chan, J.C.Y., Kioh, D.Y.Q., Yap, G.C., Lee, B.W., and Chan, E.C.Y. (2017). A novel LCMSMS method for quantitative measurement of short-chain fatty acids in human stool derivatized with (12)C- and (13)C-labelled aniline. J. Pharm. Biomed. Anal. *138*, 43–53. https://doi.org/10.1016/j.jpba.2017.01.044.

71. Curren, B., Ahmed, T., Rashid, R.B., Sebina, I., Al Amin Sikder, M., Howard, D.R., Alorro, M., Ullah, M.A., Bissell, A., Rahman, M.M., et al. (2024). A maternal high-fat diet predisposes to infant lung disease via increased neutrophil-mediated IL-6 trans-signaling. Cell Rep. *43*, 114974. https://doi.org/10.1016/j.celrep.2024.114974.

72. Ullah, M.A., Vicente, C.T., Collinson, N., Curren, B., Sikder, M.A.A., Sebina, I., Simpson, J., Varelias, A., Lindquist, J.A., Ferreira, M.A.R., and Phipps, S. (2020). PAG1 limits allergen-induced type 2 inflammation in the murine lung. Allergy *75*, 336–345. https://doi.org/10.1111/all.13991.

73. Ullah, M.A., Rittchen, S., Li, J., Hasnain, S.Z., and Phipps, S. (2021). DP1 prostanoid receptor activation increases the severity of an acute lower respiratory viral infection in mice via TNF-α-induced immunopathology. Mucosal Immunol. *14*, 963–972. https://doi.org/10.1038/s41385-021-00405-7.

74. Sebina, I., Rashid, R.B., Sikder, M.A.A., Rahman, M.M., Ahmed, T., Radford-Smith, D.E., Kotenko, S.V., Hill, G.R., Bald, T., and Phipps, S. (2022). IFN-λ Diminishes the Severity of Viral Bronchiolitis in Neonatal Mice by Limiting NADPH Oxidase-Induced PAD4-Independent NETosis. J. Immunol. *208*, 2806–2816. https://doi.org/10.4049/jimmunol.2100876.

75. Buetas, E., Jordán-López, M., López-Roldán, A., D'Auria, G., Martínez-Priego, L., De Marco, G., Carda-Diéguez, M., and Mira, A. (2024). Full-length 16S rRNA gene sequencing by PacBio improves taxonomic resolution in human microbiome samples. BMC Genom. *25*, 310. https://doi.org/10.1186/s12864-024-10213-5.

76. Callahan, B.J., McMurdie, P.J., Rosen, M.J., Han, A.W., Johnson, A.J.A., and Holmes, S.P. (2016). DADA2: High-resolution sample inference from Illumina amplicon data. Nat. Methods *13*, 581–583. https://doi.org/10.1038/nmeth.3869.

77. Bolyen, E., Rideout, J.R., Dillon, M.R., Bokulich, N.A., Abnet, C.C., Al-Ghalith, G.A., Alexander, H., Alm, E.J., Arumugam, M., Asnicar, F., et al. (2019). Reproducible, interactive, scalable and extensible microbiome data science using QIIME 2. Nat. Biotechnol. *37*, 852–857. https://doi.org/10.1038/s41587-019-0209-9.

78. Rognes, T., Flouri, T., Nichols, B., Quince, C., and Mahé, F. (2016). VSEARCH: a versatile open source tool for metagenomics. PeerJ *4*, e2584. https://doi.org/10.7717/peerj.2584.

79. Parks, D.H., Chuvochina, M., Rinke, C., Mussig, A.J., Chaumeil, P.-A., and Hugenholtz, P. (2022). GTDB: an ongoing census of bacterial and archaeal diversity through a phylogenetically consistent, rank normalized and complete genome-based taxonomy. Nucleic Acids Res. *50*, D785–D794. https://doi.org/10.1093/nar/gkab776.

80. Cao, Y., Dong, Q., Wang, D., Zhang, P., Liu, Y., and Niu, C. (2022). microbiomeMarker: an R/Bioconductor package for microbiome marker identification and visualization. Bioinformatics *38*, 4027–4029. https://doi.org/10.1093/bioinformatics/btac438.

81. McMurdie, P.J., and Holmes, S. (2013). phyloseq: An R Package for Reproducible Interactive Analysis and Graphics of Microbiome Census Data. PLoS One *8*, e61217. https://doi.org/10.1371/journal.pone.0061217.

82. Love, M.I., Huber, W., and Anders, S. (2014). Moderated estimation of fold change and dispersion for RNA-seq data with DESeq2. Genome Biol. *15*, 550. https://doi.org/10.1186/s13059-014-0550-8.

83. Benjamini, Y., and Hochberg, Y. (1995). Controlling the False Discovery Rate: A Practical and Powerful Approach to Multiple Testing. Journal of the Royal Statistical Society Series B: Statistical Methodology *57*, 289–300. https://doi.org/10.1111/j.2517-6161.1995.tb02031.x.

84. Lozupone, C., Lladser, M.E., Knights, D., Stombaugh, J., and Knight, R. (2011). UniFrac: an effective distance metric for microbial community comparison. ISME J. *5*, 169–172. https://doi.org/10.1038/ismej.2010.133.

85. Pluskal, T., Castillo, S., Villar-Briones, A., and Orešič, M. (2010). MZmine 2: Modular framework for processing, visualizing, and analyzing mass spectrometry-based molecular profile data. BMC Bioinf. *11*, 395. https://doi.org/10.1186/1471-2105-11-395.

86. Creek, D.J., Jankevics, A., Burgess, K.E.V., Breitling, R., and Barrett, M.P. (2012). IDEOM: an Excel interface for analysis of LC-MS-based metabolomics data. Bioinformatics *28*, 1048–1049. https://doi.org/10.1093/bioinformatics/bts069.

87. Zhou, H., He, K., Chen, J., and Zhang, X. (2022). LinDA: linear models for differential abundance analysis of microbiome compositional data. Genome Biol. *23*, 95. https://doi.org/10.1186/s13059-022-02655-5.

STAR★METHODS

KEY RESOURCES TABLE

REAGENT or RESOURCE	SOURCE	IDENTIFIER
Antibodies		
Anti mouse B220/CD45R-FITC	Biolegend	Cat# 103205; RRID: AB_312990; Clone: RA3-6B2
Anti mouse CD3-PerCP-Cy5.5	Biolegend	Cat# 100218; RRID: AB_1595492; Clone: 17A2
Anti mouse CD19-PerCP-Cy5.5	Biolegend	Cat# 152406; RRID: AB_2629815; Clone: 1D3/CD19
Anti mouse NK1.1-PerCP-Cy5.5	Biolegend	Cat# 108728; RRID: AB_2132705; Clone: PK136
Anti mouse SiglecH-APC	Miltenyi Biotec	Cat# 130-102-232; RRID: AB_2660878; Clone: 551.3D3
Anti mouse CD172a-AF700	Biolegend	Cat# 144022; RRID: AB_2650813; Clone: P84
Anti mouse MHCII-APC-Cy7	Biolegend	Cat# 107628; RRID: AB_2069377; Clone: M5/114.15.2
Anti mouse CD64-BV421	Biolegend	Cat# 139309; RRID: AB_2562694; Clone: X54-5/7.1
Anti mouse CD11b-BV605	Biolegend	Cat# 101237; RRID: AB_11126744 Clone: M1/70
Anti mouse XCR1-BV650	Biolegend	Cat# 148220; RRID: AB_2566410; Clone: ZET
Anti mouse CD11c-BV785	Biolegend	Cat# 117336; RRID: AB_2565268; Clone: N418
Anti mouse FceR1 alpha-PE	Biolegend	Cat# 12-5898-83; RRID: AB_466029; Clone: MAR-1
Anti mouse CD26-PE/Cyanine7	Biolegend	Cat# 137810; RRID: AB_2564312; Clone: DPP-4
Anti mouse CD4-FITC	Biolegend	Cat# 116003; RRID: AB_313688; Clone: RM4-4
Anti mouse CD8-PerCP-Cy5.5	BD Biosciences	Cat# 553036; RRID: AB_394573; Clone: 53-6.7
Anti mouse FoxP3-AF647	BD Biosciences	Cat# 560401; RRID: AB_1645201; Clone: MF23
Anti mouse TCRb-BV605	Biolegend	Cat# 109241; RRID: AB_2629563; Clone: H57-597
Anti mouse CD25-BV650	Biolegend	Cat# 102038; RRID: AB_2563060; Clone PC61
Anti mouse GATA3-PE	eBioscience	Cat# 12-996642; RRID: AB_1963600; Clone: TWAJ
Anti mouse Ly6G-FITC	BD Biosciences	Cat# 551460; RRID: AB_394207; Clone: 1A8
Anti mouse SiglecF-PE	BD Biosciences	Cat# 552126; RRID: AB_39434; Clone: E50-2440
Anti human CCR4-BV 421	BioLegend	Cat# 359414; RRID: RRID:AB_2562435: Clone: L291H4
Anti human CCR5-PE	BioLegend	Cat# 359106; RRID:AB_2562335; Clone : J418F1
Anti human CCR6-BUV395	BD Biosciences	Cat# 743356 ; RRID:AB_2741448; Clone : 11A9
Anti human CD19-PerCP-Cy5.5	Biolegend	Cat# 302230 ; RRID:AB_2073119; Clone : HIB19
Anti human CD25-PE	BioLegend	Cat# 356134 ; RRID:AB_2564145; Clone : M-A251
Anti human CD38-BUV395	BD Biosciences	Cat# 563812 ; RRID:AB_2744372; Clone : HB7
Anti human CD138-PE	BioLegend	Cat# 356504 ; RRID:AB_2561878; Clone : MI15
Anti human CD3-BV421	BD Biosciences	Cat# 563798 ; RRID:AB_2744383; Clone : SK7
Anti human CD27-PE	BioLegend	Cat# 124210 ; RRID:AB_1236459; Clone : LG.3A10
Anti human CD45RA-BUV395	BD Biosciences	Cat# 568712 ; RRID:AB_3684488; Clone : HI100
Anti human CD4-PerCP-Cy5.5	BioLegend	Cat# 300530 ; RRID:AB_893322; Clone : RPA-T4.
Anti human CD56-PE	Miltenyi	Cat# 130-113-307; RRID:AB_2733825; Clone : AF12-7H3
Anti human CD14-PerCP-Cy5.5	BioLegend	Cat# 325622 ; RRID:AB_893250; Clone : HCD14
Anti human CD8-BUV395	BD Biosciences	Cat# 563796 ; RRID:AB_2722501; Clone : RPA-T8
Anti human HLA-DR-PE	BioLegend	Cat# 307606 ; RRID:AB_314684; Clone : L243
Anti human CD123-PerCP-Cy5.5	BD Biosciences	Cat# 560904 ; RRID:AB_10563250; Clone : 7G3

(*Continued on next page*)

CellPress
OPEN ACCESS

Continued

REAGENT or RESOURCE	SOURCE	IDENTIFIER
Anti human CD11c-PE	BD Biosciences	Cat# 347637 ; RRID:AB_2129929; Clone : S-HCL-3
Anti mouse α-smooth muscle actin	Sigma	Cat# A5228-100UL; RRID: AB_262054; Clone: 1A4
Anti mouse Muc5ac	ThermoFisher	Cat# MA512178; RRID: AB_10978001
Anti human Calprotectin ELISA	Immunodiagnostik AG	Cat# A1030; Clone: MRP8/14
Anti human AAT ELISA	Immunodiagnostik AG	Cat#KR6750
Bacterial and virus strains		
Pneumonia virus of mouse (PVM)	N/A	Strain J3666
Bifidobacterium infantis	N/A	LMG 11588
Biological samples		
Infant peripheral blood mononuclear cells (PBMCs)	This study	N/A
Infant feces	This study	N/A
Murine lung	This study	N/A
Murine mediastinal lymph node	This study	N/A
Murine feces	This study	N/A
Murine serum	This study	N/A
Murine small intestine	This study	N/A
Chemicals, peptides, and recombinant proteins		
CRE	Greer	Cat# XPB46D3A4
FCS	Global Life Sciences solutions Australia P/L (T/A Cytiva)	Cat# SH30084.03
RNase A	PureLink	Cat# 12091021
12-hydroxyheptadecatrienoic acid	Cayman Chemical	Cat# 34590
Sterile zirconia beads	Daintree Scientific	Cat#11079101z; 11079110z
PCR master mix	Thermo Fisher Scientific	Cat# A25742
Taq DNA Polymerase	Invitrogen (Meridian)	Cat# BIO-21083
MgCl2	Invitrogen (Meridian) comes with Mango Taq	Cat# BIO-21083
DNTPs	Invitrogen (Bioline)	Cat# BIO-39044
Critical commercial assays		
Foxp3/Transcription Factor Staining Buffer Set	eBioscience	00-5523-00
AMPure XP beads	Beckman Coulter	Cat# A63881
SMRTbell Express Template Prep Kit 2.0	PacBio, CA, USA	101-820-200
Sequel II Binding Kit 2.1	PacBio, CA, USA	101-820-500
Sequel II Sequencing Kit 2.0	PacBio, CA, USA	101-826-100
Experimental models: Organisms/strains		
Wild type (WT) C57BL/6J mice	Animal Resources Center, WA, Australia	N/A
Deposited data		
Raw 16S rRNA sequencing data mouse studies	This study	ENA: PRJEB113220
Raw metabolomics data mouse studies	This study	https://zenodo.org/records/20184749
Oligonucleotides		
16S primers (V1-V9) Primers 27F 5′GCATC/barcode/AGRGTTYGATYMTGGCTCAG3′ 1492R 5′GCATC/barcode/RGYTACCTTGTTACGACTT3′	N/A	27F and 1492R
Software and algorithms		
FlowJo	Treestar	https://www.flowjo.com/
GraphPad Prism 9.3.1.	GraphPad	https://www.graphpad.com/

(*Continued on next page*)

Continued		
REAGENT or RESOURCE	SOURCE	IDENTIFIER
ImageJ	N/A	https://imagej.nih.gov/ij/index.html
Aperio Image Scope	Aperio, Vista	N/A
R (v4.3.1)	R Core Team	r-project.org/
QIIME2 (2022.2)	Bolyen et al., 2019	qiime2.org/
DADA2	Callahan et al., 2016	https://github.com/benjjneb/dada2
DESeq2	Love et al., 2014	https://www.bioconductor.org/packages/release/bioc/html/DESeq2.html
VSEARCH	Rognes et al., 2016	https://github.com/torognes/vsearch
Metaboanalyst 6.0	Pang Z et al., 2024	https://doi.org/10.1093/nar/gkae253
Additional resources		
Clinical trial registration	Picaud JC., 2025	https://clinicaltrials.gov/study/NCT04962594

EXPERIMENTAL MODEL AND STUDY PARTICIPANT DETAILS

Study design and population

A double-blind, randomized controlled trial with a non-randomized BF reference group was conducted in 18 centers across Belgium, France, Germany, and Spain from November 2021 to October 2024, with several planned staged endpoint analyses.[20] Infants were enrolled into the study if they were aged between 0 and 14 days and met the following criteria: healthy, full term birth ($\geq$37 weeks of gestation); birth weight $\geq$2500g and $\leq$4500g; BF infants must have been exclusively breastfed since birth and their parents must have decided to continue with exclusive breastfeeding at least through 4 months of age; and FF infants must have been exclusively consuming and tolerating a cow's milk infant formula and their parents must have independently decided not to breastfeed before study enrollment. Infants were excluded from the study for the following reasons: they had conditions requiring infant feedings other than those specified in the protocol; there was evidence of major congenital malformations (e.g., cleft palate), systemic or congenital infections (e.g., syphilis), or previous or ongoing severe laboratory or medical abnormalities; infants have received or are presently receiving medications or probiotic supplements; and ongoing or past participation in another trial since birth. The FF infants who met the eligibility criteria were randomized to the SYN or CTRL groups. A dynamic allocation algorithm with a 1:1 allocation ratio stratified by center, sex (male/female), and delivery mode (vaginal/cesarean section) was carried out using Medidata Randomization Trial Supply Management. The reference BF infants were not randomized. Given this was a double-blind trial, the identity of the specific product was blinded to everyone involved, from subjects to the contract research organization and the sponsor. Sample size calculation for the full CLARA study cohort is reported in Picaud et al.[20] based on the primary objective of growth safety. Blood samples for immunotyping analyses were sampled on a voluntary basis and were considered exploratory without additional power calculation.

Animal model of viral sLRI and pollution enhanced allergic airway inflammation

Wild type C57Bl/6J (Animal Resource Center) were housed under specific pathogen-free conditions in QIMR Berghofer Animal facility. Both male and female C57Bl/6J mice (3-4 weeks of age) were put on either a high fiber diet (SF-AIN93G, HFD) or low fiber diet (SF09-028, LFD) for 3 weeks prior to timed mating and throughout the experiment as previously described.[27] Neonates were supplemented with either control vehicle, a blend of structurally diverse HMOs (PRE: 2′FL, DFL, LNT, 3′SL, 6′SL, 3FL; 4mg/animal/day corresponding to 1.8g/L/day in infants), *B. infantis* (PRO; *B. infantis* LMG 11588, 10E6 CFU/animal/day) or a combination of HMO mix and *B. infantis* (SYN: 2′FL, DFL, LNT, 3′SL, 6′SL, 3FL; 4mg/animal/day corresponding to 1.8g/L/day in infants + *B. infantis* LMG 11588, 10E6 CFU/animal/day) once daily via intra-gastric gavage (i.g.) for 15 consecutive days starting at postnatal day (PND) 5. In one study, LFD-reared neonatal mice were supplemented with 12-HHT (0.4 μg; i.g. route) at PND 5-12 (daily) and then on alternate days until the end of the experiment. Oral administration of 12-HHT was selected to reflect the physiological gut–systemic axis engaged by synbiotic supplementation and, in the absence of established *in vivo* dosing paradigms, was guided by known BLT2-dependent biological activity of 12-HHT and related lipid mediators to test functional sufficiency rather than pharmacological optimization. To induce bronchiolitis, 10 plaque-forming units (PFU) of Pneumonia virus of mice (PVM) strain J3666, diluted in 10 μL vehicle [Dulbecco's modified Eagle's medium + 10% fetal calf serum (FCS)] was administered intra-nasally (i.n.) at PND10 under light isoflurane-induced anesthesia.[27,68] To simulate pollution enhanced allergic inflammation, mice infected with PVM at PND10 were sensitized i.n. on PND 42, 49, 56, and 63 with cockroach allergen extracts (CRE, 1 μg) in combination with particulate matter with a diameter of 2.5 micrometer or less (PM 2.5, 100 μg) in a final volume of 50 μL PBS.

Ethics and consent to participate

The studies involving humans were approved by Comite de Protection des Personnes Ile-de-France X, Geschäftsstelle Ethik- Kommission der Arztekammer Berlin K, Commissie Medische Ethiek Vrije Universiteit Brussel, Comite de Etica de la Investigacion

Provincial de Cordoba, Comite d'Ethique Hospitalo-Facultaire Universitaire de Liege, Ethikkommission an de Universitatsmedizin Rostock, Ethics Committee OG 065 AZ Sint-Jan Brugge Oostende AV, Comite d'Ethique Medicale Clinique CHC Montlegia, Ethics Committee of the Berlin Medical Association and were conducted in compliance with the Declaration of Helsinki and the International Conference on Harmonization Guidelines for Good Clinical Practice. Parent(s)/legally authorized representative(s) provided written informed consent prior to study enrollment. This trial was registered on ClinicalTrials.gov (NCT04962594) and the Consolidated Standards of Reporting Trials (CONSORT) checklist was followed for trial conduct and reporting. All animal procedures were approved by the Nestlé Animal Study Decision committee and by the QIMR Berghofer Medical Research Institute Animal Ethics Committee, under approval number P2319, in accordance with the 'Australian Code of Practice for the Care and Use of Animals for Scientific Purposes' (National Health and Medical Research Council of Australia).

METHOD DETAILS

Intervention and study product

A graphical overview of the study design of the CLARA sub-cohort is shown in Figure 1A. Total duration of the study intervention was 15 months. The study formulas were staged according to the age of the infant (1st age infant formula (IF): 0-<6 months; 2nd age Follow-up formula (FUF): 6-<12 months; 3rd age Growing-up formula (GUM): 12-15 months). Study formulas were fed orally, *ad libitum* daily and intake will have varied by infant's age, weight, and appetite. The composition of the study formula is summarized in Table S1. The SYN and CTRL were identical except that SYN was supplemented with a blend of 6 HMOs and *B. infantis* LMG 11588 plus *B. lactis* CNCM I-3446 (also known as BL818), while CTRL was not. The 6 manufactured HMOs in the SYN were 3-fucosyllactose (3FL), 2′-fucosyllactose (2′FL), 2′-3-difucosyllactose (DFL), lacto-N-tetraose (LNT), 3'sialyllactose (3′SL), and 6'sialyllactose (6′SL) and the amount and ratio between the HMOs changed from IF to FUF to GUM as the infants aged. Baseline demographics and household characteristics for the CLARA sub-cohort are summarized in Table S2.

Adverse events and medication use

Reported adverse events (AEs) and serious AEs (SAEs) were documented by each investigator as part of the eCRF including the type, incidence, severity, seriousness, and relation to feeding.[20] Data was also continuously collected from parent(s)/legal representatives using an electronic Infant Illness Diary (IID) to capture the number of occurrences and the length of time an infant experienced the following symptoms: fever, respiratory tract infections, GI symptoms, and ear symptoms. For each parent-reported diagnosis, study physicians contacted the parent(s)/legal representative and determined if the infant should be brought into the site for further evaluation (unscheduled visits). Once IID entries had been validated/confirmed by study physicians, this information was entered into the eCRF as an adverse event. Medication type and duration of use were recorded using the concomitant medication reporting form as part of the eCRF.

Fecal bifidobacterium abundance in infants

Fecal samples were collected at home by the parents using a feces tube with integrated spatula and without any buffers or additives, frozen in the home freezer (−20°C), and brought to the study site keeping the samples frozen in an icepack during transport. Samples were kept frozen at the site at −80°C until transferred every 3-4 months to the central lab for analysis. Relative *Bifidobacterium* abundance was determined using shot-gun metagenomics as previously described.[69] Strain-level resolution of *B. longum* subsp. *infantis* strains was performed as described in Capeding et al.[19]

Human blood sampling and immunotyping analyses

Blood collection at 4 months of age was used for prospective PBMC phenotype analyses based on the stool and biomarker sampling at 3 months of age. Blood was collected on a voluntary basis from CTRL (n = 39), SYN (n = 35), and breastfed infants (BF, n = 16, reference). Peripheral blood mononuclear cells (PBMCs) were isolated from venous blood and stained using a pre-validated 17-plex biomarker panel for immune cell profiling by Canopy Biosciences. PBMCs were processed within two hours after collection at study sites and loaded to ZellSafe chips that were sent to Canopy Biosciences within one month. Pre-stained biomarkers (CCR4, CCR5, CCR6) were measured within the first two days of sample reception to limit biomarker signal disturbance by the increasing autofluorescence over storage time. The remaining 14 biomarkers were stained subsequently. The whole 17-plex biomarker panel was performed by iterative multi-plex staining. Directly conjugated primary antibodies were incubated for 5 min at room temperature. A minimum of 20.000 cells were measured. The cell abundance of 29 assessed immune populations was expressed as percentage of total measured leukocytes and gating strategies are listed in Table S3. Statistical testing between randomized CTRL and SYN groups was performed using non-parametric Mann Whitney U test ($^*p < 0.05$). Non-randomized BF controls were used as reference group. No statistical test was performed between randomized and non-randomized groups due to the inherent differences in study design limiting the validity of direct comparisons.

Human fecal alpha-1-antitrypsin, calprotectin and SCFAs measurements

Fecal alpha-1-antitrypsin (AAT) and calprotectin protein levels were assessed by enzyme-linked immunosorbent assay (ELISA, Immunodiagnostik AG). For normalization, data were reported per dry stool weight. Fecal organic acids including acetic acid, propionic

acid, and butyric acid were assessed using validated liquid chromatography-tandem mass Spectrometry according to a modified published method.[70] Quantitative changes from baseline and differences between feeding groups were determined. For normalization, data were reported per dry stool weight.

Flow cytometry mouse studies

Single cell suspensions of mediastinal lymph nodes and lungs were prepared as previously described.[68,71] Briefly, mechanical disruption of these tissues was done followed by passage through 70-μm cell strainers (BD Biosciences). Geys lysis buffer was used to lyse RBCs. To differentiate between live and dead cells, the cells were incubated in Zombie Aqua (Biolegend, USA) for 15 min at 4°C. Cells were then incubated with anti-FcγRIII/II (Fc block) for 15 min at 4°C to inhibit non-specific binding. After washing, cells were stained for 30 min at 4°C with fluorescently labeled antibodies. For intracellular staining, the cells were processed with Foxp3/Transcription Factor Staining Buffer Set (eBiosciences, CA, USA) as per manufacturer instructions followed by staining with GATA3 antibody (TWAJ, PE, eBiosciences, USA) and FoxP3 antibody (MF23, BD Biosciences, USA) for 30 min at 4°C. Neutrophils (CD11c-CD11b+Ly6G+), eosinophils (CD11c-SiglecF + CD11b+Ly6G-), cDC1 (MHCII+ , CD11c+ , $CD26^+$, CD64− , CD172− , XCR1+), cDC2 (MHCII+ , CD11C+ , $CD26^+$, CD64− , CD172+ , XCR1−), pDC (B220+, CD11c+, CD11b−, Siglec-H+), Th2 (TCR-B+, CD8-, $CD4^+$, GATA3+), ILC2s (TCR-B-, GATA3+), Tregs (TCR-B+, $CD4^+$, CD8-, $CD25^+$, FoxP3+) were identified as previously described.[27,71]

Histology and immunohistochemistry mouse studies

Lung biopsies were prepared for paraffin embedding as previously described.[72] Antigen retrieval was performed on de-waxed sections by heating slides in citrate buffer for 10 min. Slides were incubated overnight with primary antibodies after blocking with goat serum (10% in PBS). Primary antibodies were diluted in 10% FCS in PBS as follows: anti-PVM (1:8000), anti-Muc5ac (1:400), α-smooth muscle actin (α-SMA; 1:1000). After washing with 0.05% Tween 20/TBS 3 times, sections were incubated with secondary antibody: anti-mouse IgG-AP for α-smooth muscle actin, anti-mouse IgG-AP for Muc5ac, and anti-rabbit IgG-AP for PVM for 1 h. Sections were counterstained with hematoxylin after slides were incubated with Fast Red (Sigma-Aldrich) and washed with distilled water. Coverslips with mounting medium were placed on the slides, and sections were scanned with ScanScope Aperio Turbo (Aperio, Vista, California). Scoring for PVM+ airway epithelial cells (AEC), airway smooth muscle (ASM) mass, and mucus hypersecretion were performed as previously described.[28,73,74]

Long read 16S rRNA sequencing and microbiome profiling in mice

DNA extraction and 16S long read sequencing from fecal samples was performed by Australian Genome Research Facility (Brisbane, Australia). PCR amplification of V1-V9 region of 16S rRNA was done for 30 cycles with denaturation (30 s at 95°C), annealing (30 s at 57°C) and extension (60 s at 72°C). Amplification was done with barcoded primers as previously described.[75] The primers and sequence were as follows:

F27 (5′GCATC/barcode/AGRGTTYGATYMTGGCTCAG3′),
R1492 (5′GCATC/barcode/RGYTACCTTGTTACGACTT3′).

Concentration and quality of amplicons and library were assessed with Qubit 1× dsDNA HS Assay Kit (Invitrogen, USA). Equimolar concentrations of amplicons were pooled, and libraries were prepared with the SMRTbell Express Template Prep Kit 2.0 (PacBio, CA, USA) as per manufacturer's instructions. AMPure PB beads were used to clean up the amplified libraries. Sequencing polymerase and primers were bound to libraries with Sequel II Binding Kit 2.1 followed by cleanup with AMPure PB beads. Sequel II Sequencing Kit 2.0 (PacBio, USA) was used for sequencing on Sequel II PacBio system. Denoising and quality filtering of PacBio HiFi full-length 16S data was performed with DADA2[76] and QIIME2.[77] VSEARCH[78] was used for consensus alignment classification against Genome Taxonomy Database (GTDB r207)[79] for classification of amplicon sequence variant (ASV). MicrobiomeMarker (v.1.8.0)[80] and phyloseq (v1.46)[81] were used to process data. DESeq2 was used to process count data and features and samples without values in at least one sample were processed with 'poscounts'.[82] p values were adjusted with Benjamini & Hochberg procedure.[83] QIIME2 (2022.2) was used to analyze Alpha and Beta diversity. Alpha diversity was measured by Pielou's evenness, Shannon's entropy, observed features. Beta diversity was calculated by weighted UniFrac distances[84] and visualized by emperor plot of the principal component analysis matrix. Significance ($p < 0.05$) in beta diversity was calculated by Permutational multivariate analysis of variance (PERMANOVA).

Untargeted metabolic profiling in mouse samples

Serum samples (20 μL) mixed with 120 μL extraction solvent (methanol with 1 μM CCP standards) were sonicated and vortexed at 4°C for 15 min. After centrifugation at maximum speed at 4°C, the supernatant was transferred to an LCMS vial. Acquisition was made on the LCMS system which consisted of Orbitrap Exploris 120 (Thermo Scientific) coupled with Vanquish Flex (Thermo Scientific). Chromatographic separation was done with SUPLECO Ascentis Express C8 HPLC column (10 cm × 2.1 mm x 2 μm) in binary gradient conditions using mobile phase A (0.1% Formic acid in HPLC grade water) and mobile phase B (0.1% formic acid in ACN). The flow rate was 0.3 mL/min flow and the gradient program was set as follows: 0min 2%B, (0min–9min) 2%B-40%B, (9min–9.5min) 40%B-95%B, (9.5min–11.5min) 95%B, (11.5 min–12 min) 95%B-2%B, (12 min–15 min) 2%B. Retention times for standards were extracted from the peak detection module of MZmine 2.53[85] or were manually examined. IDEOM[86] was used to process LCMS data. The raw

data of metabolite peak intensities was log transformed and auto scaled for principal components analysis, dendrogram construction, one-way ANOVA, correlation analysis, and heatmaps. Auto-scaled data of individual comparisons of peak intensities were used for the Upset diagram. Raw metabolomics data was uploaded into the software package Metaboanalyst 6.0 [34]. Groups were annotated as protected or susceptible to sLRI based on weight gain, which served as a core physiological marker of overall health status. Within Metaboanalyst, a 'Pattern Search' which identified metabolites that were commonly increased/decreased relative to the phenotype (in this case, protection or susceptibility) were applied. Metabolites that were higher in susceptible groups were defined as ''detrimental metabolites'' and those elevated in the disease resistant groups were defined as ''protective metabolites''. The pattern hunter feature calculated the correlation coefficient based on metabolite concentration and assigned whether they belonged to the protected or susceptible group.

QUANTIFICATION AND STATISTICAL ANALYSIS

Statistical analysis of human data

To assess differences between the randomized formula fed groups the following statistical tests were used: Non-parametric Mann Whitney U test for fecal biomarkers and immune cell populations; a linear model adjusting for baseline age and study site with compositional bias-correction[87] for microbiota at species level. Partial Pearson correlations adjusting for baseline age and study site were done to assess associations between microbiota, fecal biomarkers, and the T helper cell populations. Spearman correlations were done to assess relationships among the different immune cell populations. To control the false discovery rate due to multiple testing, the *p*-values were adjusted using the FDR method.[83] Test results were considered significant at FDR <0.10 and nominally significant at $p < 0.05$.t.

Statistical analysis of mouse data

GraphPad Prism (Version 9.3.1, GraphPad, USA) was used for statistical analysis. One way ANOVA followed by Dunnett's multiple test or Two-way ANOVA followed by Tukey's multiple comparison test were used where appropriate. *p* value of 0.05 or lower ($^{*}p < 0.05$, $^{**}p < 0.01$, $^{***}p < 0.001$) was considered statistically significant.